

HOXA10 Controls Osteoblastogenesis by Directly Activating Bone Regulatory and Phenotypic Genes[▽]

Mohammad Q. Hassan,¹ Rahul Tare,^{1†} Suk Hee Lee,¹ Matthew Mandeville,¹ Brian Weiner,¹ Martin Montecino,² Andre J. van Wijnen,¹ Janet L. Stein,¹ Gary S. Stein,¹ and Jane B. Lian^{1*}

Department of Cell Biology and Cancer Center, University of Massachusetts Medical School, Worcester, Massachusetts 01655,¹ and Departamento de Bioquímica y Biología Molecular, Facultad de Ciencias Biológicas, Universidad de Concepción, Concepción, Chile²

Received 18 August 2006/Returned for modification 4 October 2006/Accepted 9 February 2007

HOXA10 is necessary for embryonic patterning of skeletal elements, but its function in bone formation beyond this early developmental stage is unknown. Here we show that HOXA10 contributes to osteogenic lineage determination through activation of *Runx2* and directly regulates osteoblastic phenotypic genes. In response to bone morphogenic protein BMP2, *Hoxa10* is rapidly induced and functions to activate the *Runx2* transcription factor essential for bone formation. A functional element with the *Hox* core motif was characterized for the bone-related *Runx2* P1 promoter. HOXA10 also activates other osteogenic genes, including the alkaline phosphatase, osteocalcin, and bone sialoprotein genes, and temporally associates with these target gene promoters during stages of osteoblast differentiation prior to the recruitment of RUNX2. Exogenous expression and small interfering RNA knockdown studies establish that HOXA10 mediates chromatin hyperacetylation and trimethyl histone K4 (H3K4) methylation of these genes, correlating to active transcription. HOXA10 therefore contributes to early expression of osteogenic genes through chromatin remodeling. Importantly, HOXA10 can induce osteoblast genes in *Runx2* null cells, providing evidence for a direct role in mediating osteoblast differentiation independent of RUNX2. We propose that HOXA10 activates RUNX2 in mesenchymal cells, contributing to the onset of osteogenesis, and that HOXA10 subsequently supports bone formation by direct regulation of osteoblast phenotypic genes.

Patterning and development of the skeleton are complex processes involving signaling proteins and transcription factors that function as determinants for bone formation. Among the principal regulatory cascades for the development of the skeleton are *Hox* genes that determine the position and shape of a tissue element (19, 54) and the bone morphogenetic proteins (BMPs), which induce the differentiation of mesenchymal cells to osteoblast and chondroblast lineages (18, 84). BMP2 signaling leads to the induction of a number of transcription factors, including RUNX2 (28) and OSTERIX (42, 56), which are essential for bone development (34, 45, 69). Several HOX and homeodomain proteins have been identified as molecular targets of BMP-mediated gene transcription during early stages of bone formation by microarray gene expression profiling studies (3, 33). The present study was aimed at characterizing a BMP2-inducible gene, the Homeobox a10 (HOXA10) gene, as a candidate for contributing to commitment and development of the osteoblast phenotype.

Mammalian *Hox* genes (homologues of the *Drosophila* homeotic genes) encode transcription factors crucial in regional development along the anterior-posterior axis during embryogenesis (44, 64). The mouse and human genomes contain 39 *Hox* genes, which are grouped into four clusters, *Hoxa*, *Hoxb*, *Hoxc*, and *Hoxd*, positioned on four separate chromosomes in

13 paralogs (38, 44). *Hoxa10* is a member of the *Abdominal B* (Abd B) class of homeobox protein-encoding genes, representing the most 5' genes in the cluster consisting of paralog genes from *Hoxa 9* to *Hoxa 13* (4, 44, 50). The corresponding class of homeobox proteins binds preferentially to a consensus core of TTAT or TTAC, which is distinct from the TAAT homeodomain consensus core binding site recognized by MSX and DLX proteins (4). HOXA10 DNA binding is influenced by flanking sequences and the formation of complexes with HOXA10-interacting proteins of the MEIS and PBX classes of transcription factors, as well as other coregulatory proteins, such as histone deacetylase 2 (13, 51, 60, 72, 74, 81).

Several of the *Hox* genes are essential for normal skeletal development (31, 64). The nonparalogous *Hoxa10* and *Hoxd11* genes cooperate in the development of the forelimbs and axial skeleton and are required to globally pattern the mammalian skeleton (6, 7, 26, 68, 80). Inactivation of the paralogous *Hoxa10* and *Hoxd10* genes results in alterations in the formation of the forelimbs and hind limbs. *Hoxa10*^{-/-} mice revealed an active role for the gene in modeling the femur, tibia, and fibula (12, 79). Transgenic expression of HOXA10 in presomitic mesoderm of the mouse resulted in vertebrae without ribs (11). HOXA10 is expressed in the presomitic mesoderm, which develops into the axial skeleton and cooperates with other *Hox* genes (e.g., *Hoxd11*) for normal skeletal development (11, 26, 31, 64). Despite the considerable genetic evidence that HOXA10 has critical skeletal functions, target genes of HOXA10 in bone have not been identified.

In this study we have characterized HOXA10 regulation of the key osteogenic factor *Runx2*, as well as RUNX2 target genes, identifying *Hoxa10*-specific regulatory elements in pro-

* Corresponding author. Mailing address: Department of Cell Biology and Cancer Center, University of Massachusetts Medical School, 55 Lake Avenue North, Worcester, MA 01655-0106. Phone: (508) 856-5625. Fax: (508) 856-6800. E-mail: jane.lian@umassmed.edu.

† Present address: University Orthopedics, Bone and Joint Research Group, General Hospital, Southampton, United Kingdom.

[▽] Published ahead of print on 26 February 2007.

motors of the *Runx2*, osteocalcin (*OC*), alkaline phosphatase, and bone sialoprotein osteoblast-related genes. This discovery of a *Hox* regulatory factor in activating *Runx2* provides novel insights for a mechanism that regulates a transcription factor essential for bone formation (43, 58). Although *Runx2* is rapidly induced in response to BMP2 and present in developing limbs, somites, and mesenchymal condensations prior to chondrogenic and osteoblast differentiation (23, 46, 76), a Smad-responsive element has not been defined. Thus, BMP2-induced HOXA10 represents a key regulator of *Runx2* transcription during embryogenesis. Our studies also show that HOXA10 can regulate osteoblast genes independent of RUNX2. We have thus identified an additional role for HOXA10 in postnatal bone formation and maintenance of the osteoblast phenotype. We propose that HOXA10 functions in two capacities: as a component of a BMP2 signaling cascade prior to RUNX2 to mediate the developmental induction of osteogenesis and during osteoblast differentiation to regulate the temporal expression of bone phenotypic genes to drive osteoblast maturation through mechanisms involving chromatin remodeling of gene promoters.

(Brian Weiner's contribution to this paper is in fulfillment of a Worcester Polytechnic Institute undergraduate thesis project.)

MATERIALS AND METHODS

Cell cultures. C3H10T1/2 and NIH 3T3 cells were maintained in Dulbecco's minimal essential medium (MEM) (GIBCO) supplemented with 10% fetal bovine serum (FBS) (Atlanta Biologicals, Georgia). C3H10T1/2 cells were induced to osteogenesis by BMP2 (300 ng/ml). MC3T3 cells were maintained in α -MEM supplemented with 10% FBS. Primary rat osteoblast cells were isolated from calvaria according to the procedures described previously (34). The rat osteosarcoma cell line ROS 17/2.8, representing a mature osteoblast phenotype, was maintained in F-12 medium supplemented with 5% FBS (70). Cells were cultured under osteogenic conditions with MEM (GIBCO-BRL) supplemented with 10% FBS, 50 μ g of ascorbic acid/ml, and 10 mM β -glycerol phosphate. Bone marrow stromal cells were isolated from 8-week-old C57BL6 mice and cultured in MEM containing 10% FBS (29).

Runx2 null cells were isolated from calvarial tissues of mouse embryos (17.5 days postcoitum) of the *Runx2* null mouse and immortalized using mouse telomerase (TERT). Characterization of this cell line has been described previously (1). The BMP2 used in these studies was a kind gift from John Wozney (Wyeth Research, Women's Health and Musculoskeletal Biology).

Transfection and reporter assays. The *Hoxa10* expression clone containing the mouse cDNA (1.2 kb) of the *Hoxa10-1* variant (55 kDa) containing the transactivation domain was kindly provided by Richard L. Maas (Harvard Medical School, Boston, MA) (4). Transient transfections were performed in six-well plates at 50 to 70% confluence with 5 μ l of FuGENE6 transfection reagent with wild-type (WT) and deleted promoter reporter DNA according to the manufacturer's instructions (Roche, Indianapolis, IN). A tagged *Hoxa10* expression vector (pcDNA3.1-Xpress-*Hoxa10*) was constructed was used along with a *Runx2* expression vector (pcDNA3.1-HA-*Runx2*) (85) in this study. For control of expression, vector pcDNA3.1 was transfected according to the experimental condition. The following *Runx2* WT and deletion promoter reporter plasmids (21) were used: the WT *Runx2* 0.6-kb fragment and the deletion series (−490, −458, −351, −288, −128) fragments. These fragments were cloned in pGL3 basic luciferase vector (Promega, Madison WI). Cells transfected with either *Runx2* promoter luciferase or −208 *OC* promoter chloramphenicol acetyltransferase (CAT) reporter constructs along with *Hoxa10*, *Runx2*, or control vector were harvested 24 to 36 h after transfection, and all lysates were assayed for luciferase or CAT activity according to the manufacturer's instructions (Promega, Madison, WI). All results were normalized to the luciferase activity resulting from transfection of the promoterless pGL3 luciferase construct (Promega, Madison, WI). The *OC* promoter activity was assayed by using the −208-bp promoter DNA fragment from rat *OC* genes cloned in the pCAT basic vector (Promega, Madison, WI) (32). The percent CAT conversion was the average of values for six similar transfection samples.

TABLE 1. Primers for real-time PCR assays

Primer for indicated gene	Sequence
Bone marker primers (mouse)	
<i>BSP</i>	
Forward	5'-GCA CTC CAA CTG CCC AAG A-3'
Reverse	5'-TTT TGG AGC CCT GCT TTC TG-3'
<i>ALP</i>	
Forward	5'-TTG TGC CAG AGA AAG AGA GAG A-3'
Reverse	5'-GTT TCA GGG CAT TTT TCA AGG T-3'
<i>Runx2</i>	
Forward	5'-CGG CCC TCC CTG AAC TCT-3'
Reverse	5'-TGC CTG CCT GGG ATC TGT A-3'
<i>OC</i>	
Forward	5'-CTG ACA AAG CCT TCA TGT CCA A-3'
Reverse	5'-GCG GGC GAG TCT GTT CAC TA-3'
<i>Hoxa10</i>	
Forward	5'-TTC GCC GGA GAA GGA CTC-3'
Reverse	5'-TCT TTG CTG TGA GCC AGT TG-3'
Primers for ChIP (rat)	
<i>Runx2</i>	
Forward	5'-TCA GCA TTT GTA TTC TAT CCA AAT CC-3'
Reverse	5'-TGG CAT TCA GAA GGT TAT AGC TTT T-3'
<i>ALP</i>	
Forward	5'-CCT GTG CAT TTC CCA ACA CGG CGG-3'
Reverse	5'-CCA CTT CCC AGG CAG TGG AGA CAG-3'
<i>BSP</i>	
Forward	5'-GTT TAA ATG CTT AAG TCG TTT GC-3'
Reverse	5'-GGC TGT GGG TTC TCA CCA GAA A-3'
<i>OC</i>	
Forward	5'-GGC AGC CTC TGA TTG TGT CC-3'
Reverse	5'-TAT ATC CAC TGC CTG AGC GG-3'
Control 3' UTR primers for ChIP (mouse)	
<i>OC</i>	
Forward	5'-GAT CCC ATA TCA GCC AGC AC-3'
Reverse	5'-GAC TGC CCT GGA TCA CAA GT-3'
<i>Runx2</i>	
Forward	5'-CGT CCA CCT GTT CCA AAG TT-3'
Reverse	5'-GGC ATT GCC ATT TTC AGT TT-3'
<i>BSP</i>	
Forward	5'-CCT TTT CGG TGA TTG CAG TT-3'
Reverse	5'-AAG GTT GAG GGT GTC AGT GG-3'
<i>ALP</i>	
Forward	5'-TTG TTC CTC TTG CCT CAG GT-3'
Reverse	5'-TGA CAA TCA CAT GGC CTC TC-3'
Control 3' UTR primers for ChIP (rat)	
<i>OC</i>	
Forward	5'-GCA CTG CAC AGA TGT GGA AC-3'
Reverse	5'-CAG GTT TTC CCT TTC TCA GG-3'
<i>Runx2</i>	
Forward	5'-TGC TTT GCA ACC AAA TCA AG-3'
Reverse	5'-TCT GAA GGG AAG CTT TGG AA-3'
<i>BSP</i>	
Forward	5'-TGG AAG ATG CTT GAT GAC CA-3'
Reverse	5'-AAG GGG TCA GAG GAC AAG GT-3'
<i>ALP</i>	
Forward	5'-CCA GTG TGA TCC CCA GAA CT-3'
Reverse	5'-TGT CTG TAG CAA TCC CAC CA-3'

cDNA synthesis and QPCR. RNA was isolated from cultures of MC3T3, NIH 3T3, and C3H10T1/2 cells by use of TRIzol reagent (Invitrogen, Carlsbad, CA) according to the manufacturer's protocol. cDNAs were synthesized with oligo(dT) primers by use of a SuperScript first-strand cDNA synthesis kit (Invitrogen) according to the manufacturer's protocol. Gene expression was assessed by real-time quantitative PCR (RT-QPCR) using Power SYBR green PCR master mix (Applied Biosystems, California). Primers used for PCRs are listed in Table 1.

Electrophoretic mobility shift analysis (EMSA). Recombinant HOXA10 protein was translated using Promega TNT coupled with a rabbit reticulocyte lysate system (Promega). WT and mutant oligonucleotides containing the *Hoxa10*

binding site derived from the *Runx2* P1 promoter site 1 (WT, 5'G CAT TCA GAA GGT TAT AGC TTT 3'; mutant, 5'G CAT TCA GAA GGC GAT AGC TTT 3' [underlining indicates the HOXA10 binding site, and boldface indicates the mutation]) were end labeled with [γ - 32 P]ATP by use of T4 polynucleotide kinase (New England Biolabs, Massachusetts). The detailed procedures have been described previously (34). Anti-HOXA10 (N20) or a nonspecific antibody (either α -actin or normal immunoglobulin G [IgG] as indicated) (Santa Cruz) were used for the immunoshift studies. Complexes were visualized by autoradiography of a 6.5% acrylamide gel.

Immunoblotting. Each well of a six-well plate was lysed in 50 μ l lysis buffer (2% sodium dodecyl sulfate [SDS], 10 mM dithiothreitol, 10% glycerol, 12% urea, 10 mM Tris-HCl [pH 7.5], 1 mM phenylmethylsulfonyl fluoride, 1 \times protease inhibitor cocktail [Roche], 25 μ M MG132 [proteasome inhibitor from Calbiochem]) and boiled for 5 min. Equal amounts of total protein were analyzed by SDS-polyacrylamide gel electrophoresis and probed with suitable antibodies. Immunocomplexes were detected using Western Lightning chemiluminescence reagent (Perkin Elmer, Boston, MA).

Antibodies. The following antibodies were purchased from Santa Cruz Biotechnology. HOXA10 N20 (SC-17158) was for chromatin immunoprecipitation (ChIP) and EMSA, and A20 (SC-17159) was for Western blotting. RUNX2 antibodies were PEBP2 α A (M-70 [SC-10758]), PEBP2 α A (C-19 [SC-8566]), and actin (I-19 [SC-1616]). Mouse monoclonal RUNX2 antibody was a generous gift from Yoshi Ito and Kosei Ito (National University, Singapore, Republic of Singapore). Anti-hyperacetylated histone H4 (Penta) and anti-trimethyl histone H3 (Lys4), clone MC315, were purchased from Upstate Cell Signaling Solutions (Charlottesville, VA). The mouse monoclonal anti-Xpress antibody was obtained from Invitrogen (Carlsbad, CA). Mouse monoclonal antibody against RNA polymerase II (Pol II) (clone 8WG16) was obtained from Covance (Princeton, NJ) and used in ChIP studies.

ChIP assays. The procedure for ChIP in primary rat osteoblasts has already been described (34). Control primer pairs from 3' untranslated regions (UTR) of the genes were used to verify specific and nonspecific binding of DNA fragments (Table 1). IgG antibody was used as a control for nonspecific pull-down of immunocomplexes. Sequential ChIP studies were performed using the primary pull-down from one antibody, which was divided into equal aliquots for the second pull-down with antibodies specific for coregulatory molecules. Instead of being eluted in 1% SDS and 100 mM Na₂HCO₃ after cross-linking and washing, immunocomplexes were eluted in 10 mM dithiothreitol. The eluate was further diluted 1:40 in ChIP dilution buffer (0.01% SDS, 1.1% Triton X-100, 1.2 mM EDTA, 167 mM Tris-HCl [pH 8.1], 167 mM NaCl) and used for the second immunoprecipitations. Aliquots (2 to 3 μ l) of DNA samples from different pull-downs were assayed by either radioactive labeling or RT-QPCR using Power SYBR green PCR master mix (Applied Biosystems, California) for the detection of specific DNA fragments with primers in the proximal promoters of bone-related genes that encompass the *Hoxa10* binding sites (Table 1).

Immunohistochemistry and immunofluorescence. Long bones from normal newborn mice were fixed with 4% paraformaldehyde in 0.1 M cacodylate buffer, pH 7.4, for 48 h, dehydrated, and embedded in paraffin by standard procedures. Paraffin-embedded tissues (5- μ m sections) were immunoperoxidase labeled and blocked by 0.3% H₂O₂ in absolute methanol for 30 min at room temperature. To reveal antigens, sections were put in a 1 mM Tris solution, pH 9.0, supplemented with 0.5 mM EGTA. The sections for RUNX2 immunohistochemistry were heated in a microwave oven for 10 min after EGTA treatment, while a normal steaming antigen retrieval method was used for HOXA10. Nonspecific immunoglobulin binding was prevented by incubating the sections in 50 mM NH₄Cl for 30 min followed by blocking with phosphate-buffered saline supplemented with 1% bovine serum albumin, 0.05% saponin, and 0.2% gelatin. Serial sections were incubated overnight at 4°C with anti-rabbit RUNX2 (M-70 and C-19) or anti-goat HOXA10 (N20) antibody diluted (1:100) in phosphate-buffered saline supplemented with 0.1% bovine serum albumin and 0.3% Triton X-100. Equal amounts of the respective blocking peptides (2 μ g/ml) for HOXA10 and RUNX2 were also used. Normal IgG was used as a nonspecific control. Immunolabeling controls were performed by using antibodies preabsorbed with immunizing peptides. Labeling was visualized with the horseradish peroxidase-conjugated secondary antibody (P448, 1:200; Dako).

MC3T3 cells were plated at a density of 0.6×10^5 cells/well on gelatin-coated coverslips in six-well plates. Cells were processed for in situ immunofluorescence analyses, which were carried out as described previously (39). HOXA10 was detected by a goat polyclonal antibody at a dilution of 1:100 (Santa Cruz Biotechnology). The secondary antibody used was Alexa 488-anti-goat antibody (Molecular Probes) at a dilution of 1:800. For overexpressed HOXA10 protein, HeLa cells at 0.5×10^5 cells/well on gelatin-coated coverslips were transfected with 0.5 μ g of *Hoxa10* expression construct, and 24 h after transfection the

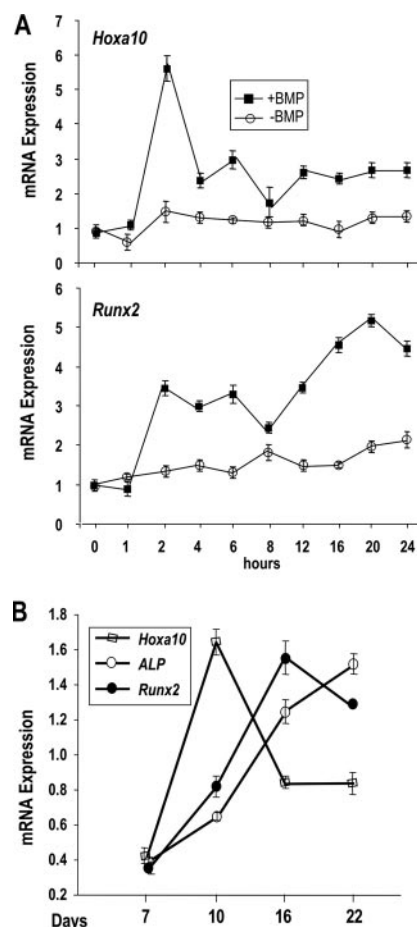


FIG. 1. *Hoxa10* expression in relation to osteogenic differentiation. (A) Premyogenic C2C12 cells were treated with 100 ng/ml BMP2 for 24 h. Total RNA was isolated at different time points (0, 1, 2, 4, 6, 8, 12, 16, 20, and 24 h). Five micrograms of total RNA was reverse transcribed with oligo(dT) primer and amplified (RT-QPCR) by gene-specific primers. (Top) *Hoxa10* expression (+BMP, -BMP) was normalized to *Gapdh* expression (+BMP, -BMP), and relative transcript levels were plotted; (bottom) the induction of *Runx2* expression with BMP2 treatment is shown for the same time course. Error bars represent triplicate analyses of each sample from two independent experiments. (B) Temporal expression of *Hoxa10* and the osteogenic markers *Runx2* and *ALP* during MC3T3 cell growth and differentiation. cDNAs from different time points were amplified using bone-specific gene primers (Table 1). Expression values from RT-QPCR were normalized to *Gapdh* values. Error bars represent triplicate sample analyses from one experiment. Independent experiments exhibited similar temporal expressions (data not shown).

coverslip was processed for immunofluorescence study (39). Xpress-HOXA10 was detected by a mouse monoclonal antibody against the Xpress tag at a dilution of 1:3,000 (Invitrogen). The secondary antibody used was Alexa 568-anti-mouse antibody (Molecular Probes, Eugene, OR) at a dilution of 1:800. Slides were examined on a Zeiss Axioplan 2 microscope fitted with epifluorescence (Carl Zeiss, Jena, Germany) attached to a charge-coupled-device camera. Images were saved and processed using Metamorph imaging software, version 6.1 (Universal Imaging, Downingtown, PA).

RNA interference (RNAi) of *Hoxa10*. The mouse MC3T3-E1 osteoblastic cells at 30 to 50% confluence were transfected using Oligofectamine (Invitrogen Life Technologies) with small interfering RNA (siRNA) duplexes specific for murine *Hoxa10* (r(CCA AAU UAU CCC ACA ACA A)dTdT and r(UUG UUG UGG GAU AAU UUG G)dCdG obtained from QIAGEN Inc. (Stanford, CA). Six different sets of siRNA duplexes at different concentrations were used to eval-

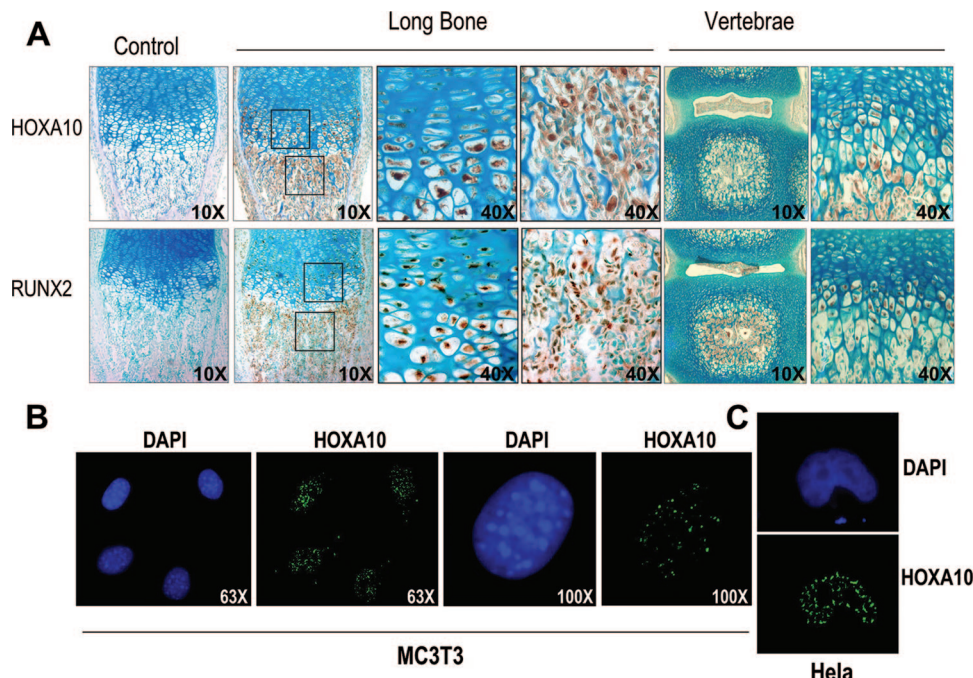


FIG. 2. Coexpression of HOXA10 and RUNX2 in vivo and in vitro. (A) HOXA10 and RUNX2 are visualized in hypertrophic chondrocytes and osteoblast lineage cells in long bones and vertebrae as indicated. Immunohistochemistry was performed using anti-HOXA10 antibody and anti-RUNX2 antibody. For nonspecific controls, normal rabbit IgG was substituted for primary antibody, and blocking peptides specific for the HOXA10 and RUNX2 antibodies were used. Bone and vertebra sections are shown at $\times 10$ and $\times 40$ magnification as indicated for the boxed areas at the growth plate and the primary spongiosa. Trabeculae show robust expression of both proteins in surface osteoblasts. The first column shows peptide blocking controls (magnification, $\times 10$). (B) In situ immunofluorescence examination of endogenous HOXA10 protein in MC3T3 cells to demonstrate nuclear staining with few cytoplasmic foci using the Santa Cruz antibody. (C) Nuclear localization of transfected Xpress-tagged HOXA10 is also observed for HeLa cells detected with anti-Xpress antibody (see Materials and Methods). DAPI, 4',6'-diamidino-2-phenylindole.

uate the target specificity and knockdown efficiency. The cells were also transfected with control siRNA duplexes specific for green fluorescent protein by use of the same concentrations to check the transfection efficiency. The siRNA experiment was carried out for 72 h. Total RNA and proteins from the specific siRNA oligonucleotide-treated, untreated, Oligofectamine-treated and nonspecific-oligonucleotide-treated cells were analyzed by Western blotting and RT-QPCR. To study chromatin modifications after *Hoxa10* siRNA treatment, cells were harvested 72 h posttransfection and used for immunoprecipitation with trimethyl histone H3K4 and hyperacetylated H4 antibody for ChIP analyses.

RESULTS

***Hoxa10* is a BMP2-responsive gene correlating to the induction of *Runx2*-mediated osteogenesis.** *Hoxa10* was identified as an early BMP2-responsive gene in an Affymetrix cDNA profiling study of BMP2-mediated osteogenic induction of premyogenic C2C12 cells (3). During the 24-h time course, *Hoxa10* expression clustered into a group of genes in which the osteogenic transcription factor *Runx2* was also present. We carried out independent experiments in this study and quantitated gene expression by RT-QPCR to validate the microarray report (Fig. 1A). Both *Hoxa10* and *Runx2* mRNAs are present at very low levels in untreated cells, immediately upregulated by BMP2 within 2 h, and then partly downregulated, but they exhibit a second spike at 6 h. After the 8-h commitment point to osteogenesis, when bone phenotypic markers (alkaline phosphatase and OC) are expressed (3), *Hoxa10* mRNA remains at a steady state, while *Runx2* continuously increases.

To further evaluate the expression of *Hoxa10* and *Runx2*

during the development of the osteoblast phenotype, we examined the temporal expression of *Hoxa10* during the differentiation of osteoprogenitor MC3T3 cells. *Hoxa10* is endogenously expressed at low levels in the proliferating cells (day 7) and is induced four- to fivefold upon the maturation of the phenotype, concurrent with cellular multilayering (day 10 in this experiment) (Fig. 1B). Peak mRNA expression levels of *Hoxa10* are transient and downregulated by 50% by day 16, the onset of mineral deposition in MC3T3 cells. Expression of *Runx2* and alkaline phosphatase phenotypic genes continuously increases during differentiation. These observations suggest that *Hoxa10* expression is important at the early stages of osteoblast differentiation. We further showed that either treatment of pluripotent C3H10T1/2 cells with BMP2 or growth of adherent bone marrow cells in osteogenic media results in a twofold increase in *Hoxa10* concomitant with the expression of the osteoblast phenotype (data not shown). These studies implicate HOXA10 in establishing early events in the development of the osteoblast phenotype.

To appreciate the role of HOXA10 in osteogenesis in vivo, we examined its expression in bone cell populations in situ in relation to endochondral bone formation and skeletal development. Sections of long bones and vertebrae from newborn mice were treated with specific antibodies to detect RUNX2 and HOXA10 (Fig. 2). We found strong expression of HOXA10 in the periosteum, the hypertrophic chondrocyte zone of the growth plate, and osteoblasts on all bone surfaces.

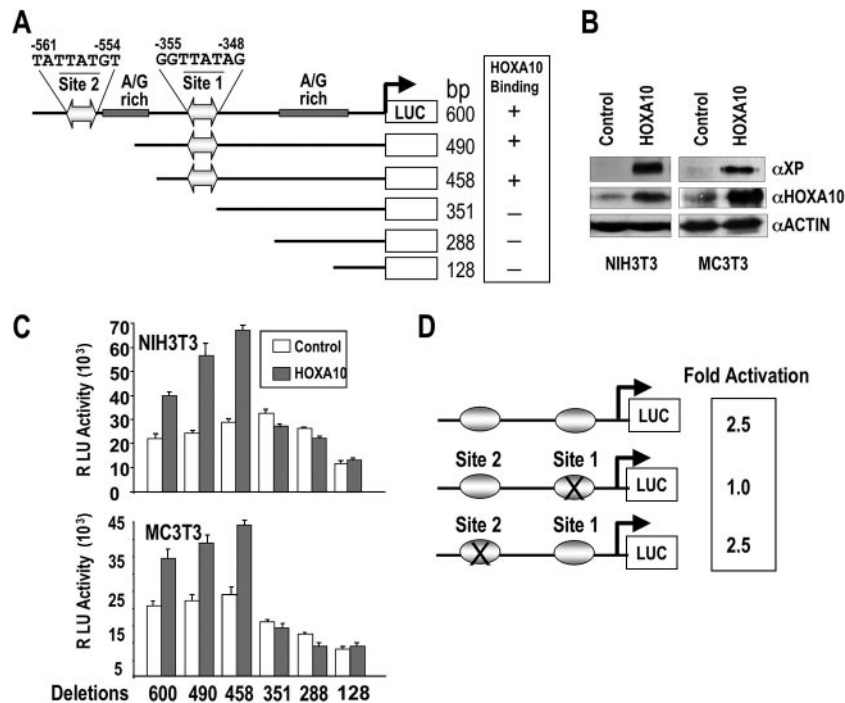


FIG. 3. HOXA10 directly regulates *Runx2* promoter activity and transcription. (A) Schematic representation of the deletions of the 0.6-kb *Runx2* promoter with the firefly luciferase reporter gene. The full-length 0.6-kb promoter contains two *Hoxa10* putative binding sites (site 1 and site 2) having the core TTAT motifs. Deletion clones -490- and -458-Luc contain only site 1, whereas clones -351-, -288-, and -108-Luc are devoid of *Hoxa10* binding sites. (B) Western blots of endogenous and exogenous HOXA10 protein levels in nonosseous (NIH 3T3) and osseous (MC3T3) cells. For detection of endogenous and exogenous HOXA10 protein, anti-HOXA10 (N20; Santa Cruz Biotech Inc.) was used. α , anti-XP. (C) A functional *Hoxa10* resides in the proximal *Runx2* promoter. *Runx2* promoter deletion mutant constructs were cotransfected with 400 ng of either backbone vector (control representing basal promoter activity [open bars]) or *Hoxa10* expression construct (treated [solid bars]). *Runx2* promoter activities are calculated from relative luciferase values for both NIH 3T3 and MC3T3 cells. All transfections were performed in triplicate. RLU, relative light units. (D) Two nucleotide mutations (TTAT to CGAT) were constructed in the distal (site 2) and proximal (site 1) *Hoxa10* binding motifs in the 0.6-kb *Runx2* P1 promoter as illustrated. *Hoxa10*-mediated activation for WT/mutant is indicated.

RUNX2 was also expressed in these cell populations. Weak expressions of HOXA10 and RUNX2 were found in the flat-tended cells that represent the prehypertrophic chondrocyte phenotype. It is noteworthy that both HOXA10 and RUNX2 were absent from the epiphyseal chondrocytes that represent permanent hyaline cartilage. Similar observations were made for vertebrae tissue. We conclude from these studies that RUNX2 and HOXA10 are expressed in osteogenic lineage cells and maturing chondrocytes at the growth plate in both the axial and appendicular skeletons.

While most immunohistochemical staining is nuclear, some hypertrophic chondrocytes and osteoblasts have cytoplasmic staining representing either background or specific HOXA10 staining. To address a potential artifact of cytoplasmic staining, we examined the endogenous localization of HOXA10 by in situ immunofluorescence in isolated osteoblasts. Punctate nuclear staining was observed, with a few foci detected in the cytoplasm of MC3T3 cells (Fig. 2B). However, 100% nuclear localization was observed with exogenously expressed HOXA10 protein in HeLa cells by use of the Xpress tag antibody (Fig. 2C). These findings indicate that the localization of the HOXA10 isoform with transactivation activity is nuclear.

The coordinate BMP2 induction of *Hoxa10* and *Runx2* in response to BMP2-induced osteogenesis in several cell models, taken together with the profiles of expression of these genes

during the maturation of MC3T3 cells as well as their coexpression in osteogenic lineage cells, suggests a functional relationship between RUNX2 and HOXA10.

The P1 bone-related promoter of *Runx2* and the endogenous *Runx2* gene are regulated by HOXA10. As activating signals on the *Runx2* promoter during early stages of embryonic development are limited, we pursued the characterization of a *Hoxa10* regulatory element in the bone-related *Runx2* P1 promoter. Examination of the *Runx2* 0.6-kb promoter, which has been studied for its regulation in osseous and nonosseous cells, revealed the presence of three putative *Hox* consensus sequences. Two TTAT-containing core sequences (4, 24) and one sequence with a TTAC core (72), which binds HOXA9 well but HOXA10 with a low frequency (4, 73), are present in the proximal promoter (Fig. 3A). These sequences differ from the TAAT binding site for homeodomain proteins of the MSX and DLX classes (34, 45). To identify the HOXA10-responsive regulatory element(s) in the *Runx2* gene, deletion mutation analyses were performed with both NIH 3T3 (nonosseous) and MC3T3 (osseous) cells cotransfected with *Runx2* promoter deletion fragments and HOXA10. The endogenous protein levels of HOXA10 are slightly higher in the MC3T3 preosteoblasts than in the NIH 3T3 fibroblasts (Fig. 3B, control lanes) which may be contributing to the basal expression of the promoter constructs in MC3T3 cells, where the -351 fragment is

reduced 20% (Fig. 3C). In the presence of exogenous HOXA10, a 2- to 2.5-fold increase in promoter activity of the -600, -490, and -458 fragments is observed, suggesting that the proximal TTAT site 1 is sufficient for HOXA10 regulation of *Runx2* (Fig. 3C). Furthermore, complete loss of HOXA10 responsiveness occurs with the -351 *Runx2*-Luc fragment, which lacks the putative site 1 for HOXA10 binding. Furthermore, mutation of site 1 blocked HOXA10-mediated transcriptional activation (Fig. 3D). The site 2 mutation had no effect on HOXA10 induction of *Runx2*, i.e., the construct retained the same 2.5-fold activation level as the WT. The TTAC core site, located at -420/-417, cannot be functional, as the site 1 mutation showed no HOXA10-induced change in promoter activity. Taken together, these results are consistent with the location of a functional *Hoxa10* site in the proximal promoter fragment at -353/-351, a regulatory element mediating HOXA10 activation of the *Runx2* P1 promoter.

Sequence-specific binding of HOXA10 to the proximal regulatory motif was validated in EMSA by WT and mutant oligonucleotide binding studies (Fig. 4A and B). Confirming the mutation studies, site 2 does not form a HOX protein-DNA complex with osteoblast nuclear extracts (Fig. 4B). In contrast, site 1 binds in vitro-transcribed and -translated (IVTT) HOXA10 protein and HOXA10 from nuclear extracts of osteoblasts, as indicated by antibody supershifts (Fig. 4B). To rule out the possibility of redundant HOX protein binding to site 1 because other HOX factors are expressed in osteoblasts (20, 30), we further examined the interaction of other paralogous HOX proteins expressed in MC3T3 cells with *Runx2* site 1. Antibody specificities were established by testing IVTT HOXA10 protein bound to probe with supershift analyses using antibodies specific to other Abd B class proteins. None of these antibodies cross-reacted with HOXA10 (Fig. 4C, left panel), nor did they supershift/block shift the HOXA10 complex from nuclear extracts bound to *Runx2* site 1 (Fig. 4C, right panel). In conclusion, the deletion and site-directed mutagenesis of putative *Hox* elements in the 0.6-kb *Runx2* promoter demonstrates that HOXA10 protein binds preferentially to the *Runx2* TTAT site 1.

To address the biological significance of the HOXA10-mediated positive regulation of the *Runx2* gene at the onset of osteoblast differentiation, cellular levels of HOXA10 were inhibited by siRNA knockdown in two osteogenic cell models. Preosteoblastic MC3T3 cells were treated with several *Hoxa10* siRNA duplex oligonucleotides for 72 h, which resulted in the inhibition of HOXA10 cellular protein levels compared with the nonsilencing duplex control. Figure 5A shows results for two siRNAs, one of which only modestly decreased HOXA10 protein (siRNA2; decrease of 10 to 15% from densitometry measurements), while siRNA1 exhibited a robust dose-dependent inhibitory effect on HOXA10 and also caused a significant dose-related decrease in RUNX2 protein (Fig. 5B).

The potency of HOXA10 in regulating *Runx2* at the onset of BMP2-induced osteogenesis was examined with C2C12 cells (Fig. 5C). Cells were first treated with siRNA for 48 h, which was followed by BMP2 for 2 h. *Hoxa10* siRNA resulted in a 50% knockdown of *Hoxa10*, a decrease which prevented the twofold BMP2 induction of *Hoxa10* mRNA in the control (absence of *Hoxa10* siRNA). *Runx2* was reduced nearly 75% by *Hoxa10* siRNA in the absence of BMP2. In the presence of

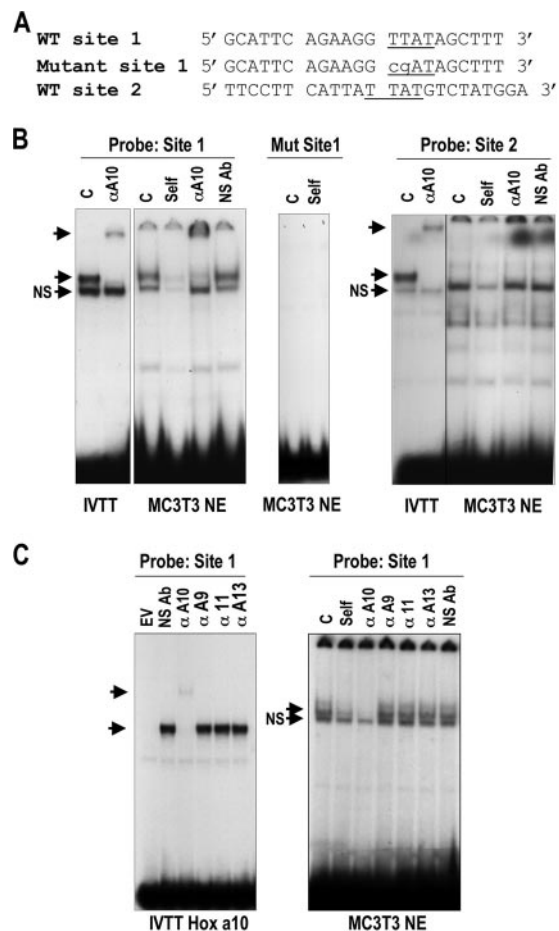


FIG. 4. Specificity of the *Hoxa10* site 1 for HOXA10 interactions. (A) Oligonucleotide sequences are shown for the WT and the *Hoxa10* site mutations and compared to that for the mouse consensus optimal *Hoxa10* binding site (4). Underlining indicates the core binding site; lowercase indicates mutant nucleotides. (B) DNA binding activity of HOXA10 is demonstrated by EMSA. Ten femtomoles of labeled double-stranded oligonucleotides derived from the WT or mutant (Mut) probe as indicated was incubated with 2 μ l of IVTT HOXA10 or 5 μ g of MC3T3 nuclear extract (NE). Self-competition (Self), antibody supershift, and nonspecific antibody (NS Ab) controls are shown. The mutant double-stranded oligonucleotide for *Hoxa10* does not bind nuclear proteins. The top unlabeled arrows indicate the supershifted band; the lower unlabeled arrows show the position of the HOXA10-specific band, below which is a nonspecific complex (arrows labeled NS). α , anti-; C, control. (C) IVTT of indicated HOX proteins is complexed with the *Hox* site 1 in *Runx2* to show the specificity of the HOXA10 antibody. Nuclear extracts of MC3T3 osteoblasts were used in EMSA studies to show the specificity of the HOXA10 interaction (arrow) with the site 1 *Runx2* probe. GFP, green fluorescent protein; EV, empty vector.

BMP2 and *Hoxa10* siRNA, *Runx2* was not induced to a level over that seen for the control. However, the inhibition was less (33% decrease) than in the absence of BMP2 (>50% decrease). This finding is likely the consequence of BMP2 induction of other transcription factors that can upregulate *Runx2*. Thus, we were prompted to examine levels of *Dlx3*, a BMP2 early response gene in this cell model (35). *Dlx3* was induced over the control in the presence of *Hoxa10* siRNA and BMP2 (data not shown). These studies define HOXA10 as a signifi-

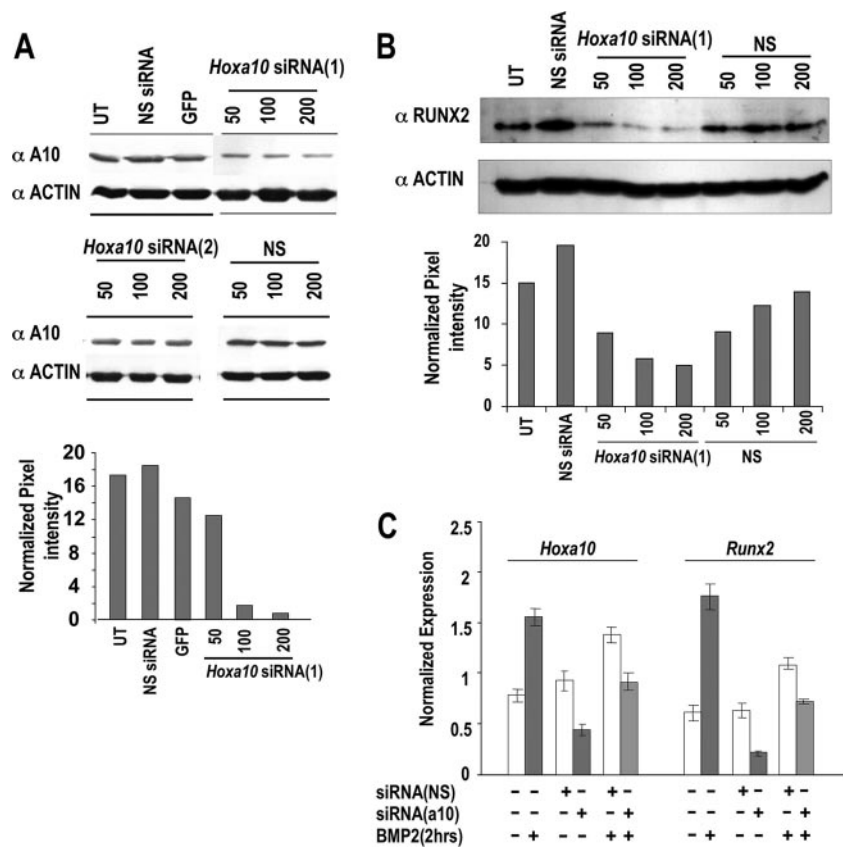


FIG. 5. RNAi of *Hoxa10* in MC3T3 and C2C12 cells inhibits *Runx2* and osteogenic gene expression. (A) Knockdown of *Hoxa10* in MC3T3-E1 cells by two sets of *Hoxa10* siRNA duplexes and nonspecific controls (NS). The lower panel shows densitometric quantitation of HOXA10 knockdown when cells were isolated 72 h after siRNA treatment. (B) Preosteoblast MC3T3 cells at 30 to 50% confluence were transfected with siRNA1 specific for murine *Hoxa10* at different concentrations (50, 100, and 200 nM). (Top) The Western blot shows the knockdown of RUNX2 protein upon treatment with *Hoxa10*-specific siRNA duplexes. UT, untransfected; NS, nonsilencing duplexes (used as controls). Densitometry shows reductions of RUNX2 protein upon knockdown of *Hoxa10*. (C) C2C12 cells were plated on day 0 at 30 to 40% confluence and treated with *Hoxa10* siRNA or nonspecific siRNA [siRNA(NS)] (100 nM) for 48 h. After the medium was changed, BMP2 (100 ng/ml) was added to induce *Hoxa10* and *Runx2* for 2 h. mRNA levels were assayed by RT-QPCR. White bars represent the control for the treatment as indicated. GFP, green fluorescent protein; α, anti-.

cant regulator of *Runx2* transcriptional activity and gene expression.

Functional recruitment of HOXA10 to promoters of *Runx2* and other osteoblast-related genes. To gain further insight into the in vivo regulation of *Runx2* transcription by HOXA10 during the development of the osteoblast phenotype, we performed ChIP assays with primary rat calvarial osteoblasts, which undergo a well-documented sequence of maturation stages (59). Western blot analysis for RUNX2 and HOXA10 protein levels during the differentiation time course shows that a low basal level of HOXA10 protein is present in proliferative osteoblasts (day 4), while RUNX2 protein is not observed until day 6 (Fig. 6A). When bone-like nodules form on day 10, HOXA10 is upregulated twofold, increases again on day 12, and remains at a constitutive level into the mineralization stage (day 20). RUNX2 protein levels increase continuously during osteoblast maturation but are reduced on day 20 (heavily mineralized cultures). These findings emphasize that HOXA10 is present in osteoprogenitors prior to RUNX2 protein appearance and that HOXA10 may function throughout differentiation.

The timing of recruitment of HOXA10 to the *Runx2* gene in relation to transcription was determined by ChIP assays at the indicated days during differentiation (Fig. 6B). Trace levels of HOXA10 above those for the IgG control were observed on days 4 and 5 in different experiments. Consistently, we found that RNA Pol II and HOXA10 were robustly associated with the promoter, beginning on day 6, when RUNX2 protein was first detected in this experiment (Fig. 6B). This coordinate occupancy was reproducible over multiple time courses (data not shown). HOXA10 remained bound to the *Runx2* promoter but dissociated on day 20, the late mineralization stage, a finding consistent with decreased RUNX2 protein levels in the cells (Fig. 6A) and decreased RNA Pol II association with the promoter (Fig. 6B). On the other hand, RUNX2 association with its own promoter gradually increased from day 6 to day 20 in late mineralization, reflecting its role in maintaining physiologic transcription by autoregulation (21). Thus, HOXA10 contributes both to the significant activation of *Runx2* expression throughout the early stages of osteoblastogenesis and to the regulation of physiologic levels in mature osteoblasts by dissociation from the *Runx2* promoter.

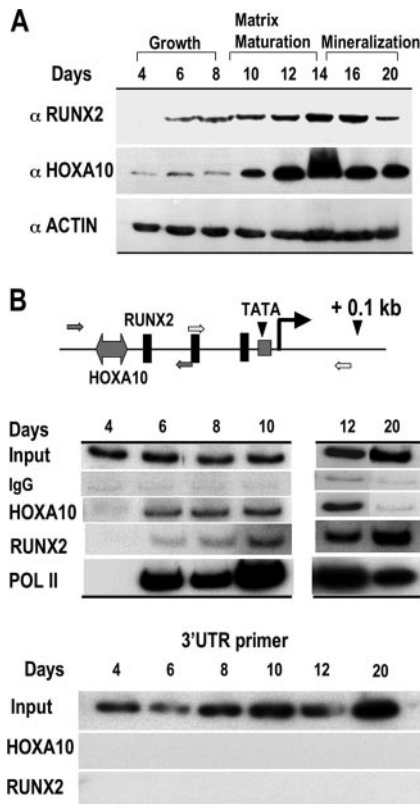


FIG. 6. HOXA10 protein and recruitment to the *Runx2* promoter in primary calvarial cells during osteoblast growth and differentiation. (A) Western blot analyses for RUNX2 and HOXA10 protein expression are shown during stages of growth and differentiation of isolated primary calvarial osteoblasts as indicated (antibody information is provided in Materials and Methods). Protein profiles of actin demonstrate equivalent amounts of total protein loaded in the gel. (B) ChIP studies of the *Runx2* proximal promoter locus during growth and differentiation. The top panel illustrates the positions of regulatory elements and primers used to amplify the *Runx2* promoter-specific DNA fragments. Open arrow, RNA Pol II; solid arrow, HOXA10 and RUNX2 occupancy. For the middle panel, ChIP analysis was performed on the indicated days with antibodies for HOXA10, RUNX2, or RNA Pol II (see Materials and Methods). One percent of the soluble chromatin fraction was taken as the input fraction. IgG is shown as an antibody control. The lower panel shows the control for ChIP primer specificity.

ChIP studies allow for assays of transcription factors associated with different promoters in the same sample. We therefore examined the promoters of several osteoblast genes for potential *Hoxa10* binding sites and designed primers to amplify the DNA of the appropriate promoter domain. Table 2 shows the putative sequences. We examined the direct regulation of the osteoblast-specific *OC* gene, which is highly regulated by RUNX2 (40). A *Hox* binding site was located in the proximal -208 promoter segment, which exhibits tissue-restricted expression (37) (Fig. 7A). Using a -208 OC-CAT reporter construct, we found a two- to threefold increase in promoter activity in response to HOXA10 in multiple experiments (Fig. 7B). By ChIP analysis (Fig. 7C), we found that HOXA10 is associated with *OC* chromatin 24 h prior to RUNX2 association. During osteoblast differentiation, both HOXA10 and RUNX2 binding were enhanced on days 8 and 9, when *OC* mRNA first began to accumulate (Fig. 7D), consistent with

increased Pol II binding on day 9 (Fig. 7C). After this initial induction of *OC*, HOXA10 association with the *OC* promoter diminished in the matrix maturation and mineralization stages, while RUNX2 remained present on *OC* chromatin. The coordinate increase in HOXA10 and RUNX2 binding to *OC* prompted us to examine the combined effects of HOXA10 and RUNX2 on *OC* promoter activity. We found an additive effect on promoter activity as a result of the coexpression of the factors (Fig. 7B), suggesting that the *Hoxa10* and *Runx2* regulatory elements function independently on the *OC* promoter, not synergistically. Taken together, these results demonstrate HOXA10 supports the regulation of *OC* expression earlier than RUNX2 and significantly contributes to *OC*-induced mRNA.

We also examined the promoters for alkaline phosphatase (*ALP*) and bone sialoprotein (*BSP*) and found *Hoxa10*-regulatory elements (Table 2 and Fig. 8). In proliferating primary osteoblasts, *ALP* (Fig. 8A) and *BSP* (Fig. 8B) are expressed, but at low levels. Association of HOXA10 with the *ALP* and *BSP* promoters was confirmed by ChIP assay with the osteoprogenitor cells (day 4) as well as with postproliferative mature osteoblasts (days 12 and 20). Interestingly, HOXA10 association with the promoter of *ALP*, the early marker of osteoblasts, was most prominent on day 4 and reduced on day 20, when *ALP* mRNA is downregulated. In contrast, both HOXA10 binding to the *BSP* promoter and *BSP* expression (mRNA) increased during differentiation. These observations suggest that HOXA10 directly regulates genes independent of RUNX2 binding.

These ChIP studies reveal that the recruitment of RUNX2 to most gene promoters continuously increases during differentiation, with similar profiles in each case (Fig. 8C). Figure 8C summarizes the profiles (from densitometry measurements of the ChIPs) of RUNX2 and HOXA10 association with four gene promoters. In contrast to RUNX2, HOXA10 has distinct profiles of association/dissociation with individual gene promoters during differentiation. It is notable that HOXA10 association to the gene promoters is critical to gene regulation independent of HOXA10 cellular levels (Fig. 8C, left panel). These differences may reflect very dynamic functional characteristics of HOXA10 promoter binding in relation to the regulation of the transcription of osteoblast genes at stages of osteoblast phenotype development. We conclude from these studies that *Hoxa10* functional elements are present in multiple osteoblast genes, including the *OC*, bone sialoprotein, and alkaline phosphatase genes, contributing to their regulated expression.

HOXA10 regulates osteoblast genes both dependent on (in MC3T3 cells) and independent of (in *Runx2* null cells) RUNX2. The ChIP studies (Fig. 6, 7, and 8) suggest that HOXA10 may regulate osteoblast genes that are significant functional components of bone, either synergistically, by increasing *Runx2* expression, or directly, through *Hox* regulatory motifs. We therefore examined the consequences of the depletion of *Hoxa10* on the endogenous expression of these skeletal markers of osteoblast differentiation by RT-QPCR (Fig. 9A). MC3T3 cells were treated with *Hoxa10* siRNA for 48 h, which reduced *Runx2* gene expression threefold. Dose-dependent decreases of the early osteoblast markers *ALP* and *BSP* were also observed, as was a twofold reduction in *OC* mRNA. Exoge-

TABLE 2. HOXA10 binding motifs in bone-specific promoters

Promoter	Nucleotide at indicated position ^a											Binding	Functional activity
	-4	-3	-2	-1	1	2	3	4	5	6	7		
<i>Hoxa10</i> consensus	A	A	T	T	T	T	A	T	T	A	C		
<i>Runx2</i> (mouse) ^e	A	A	G	G	T	T	A	T	A	G	C ^b	++	+
<i>Runx2</i> (rat) ^e	T	T	C	A	T	T	A	T	T	A	T ^c	+	-
	A	A	C	C	T	T	A	C	A	G	G ^d	-	-
<i>OC</i> (mouse)	C	T	G	C	T	T	A	C	A	T	C		
<i>OC</i> (rat)	C	T	G	C	T	T	A	C	A	T	T		
<i>BSP</i> (mouse)	T	A	T	T	T	T	A	T	T	T	G		
<i>BSP</i> (rat)	T	A	G	T	T	T	A	T	T	T	T		
	T	T	A	T	T	T	A	T	A	G	A		
<i>ALP</i> (mouse)	C	T	G	C	T	T	A	T	G	A	A		
<i>ALP</i> (rat)	G	T	C	A	T	T	A	T	A	A	C		
	T	C	G	T	T	T	A	T	G	C	A		
	T	T	A	C	T	T	A	T	A	G	G		

^a Osteoblast gene sequences were obtained from the NCBI database. HOXA10-allowed nucleotides (-4 to -1 and 5 to 7) outside the core (1, T; 2, T; 3, A; 4, T or C) are as follows for the indicated positions, as detailed in the work of Benson et al. (4): -1, T>G; -2, T>G; -3, A>T>G; -4, A>G = T; 5, T>G>A; 6, A>G>C; 7, C>A = G. HOXA9 can bind to TTAC as well as to TTAT sites, as shown by Shen et al. (72-74).
^b *Runx2* functional *Hoxa10* sequence (site 1) (Fig. 3 and 4).
^c HOXA10 binds IVTT protein but not in nuclear extracts and is nonresponsive to *Runx2* site 2 (Fig. 3 and 4).
^d Uncharacterized *Runx2* binding site with TTAC motif (-419/-416).
^e The corresponding HOXA10 binding site indicated in nucleotides across species and obtained for different bone marker genes (*Runx2*, *OC*, *BSP*, and *ALP*).

nous expression of HOXA10 in MC3T3 cells (Fig. 9B) shows that *Runx2* and *ALP* expression is increased twofold, while the mature osteoblast-related genes *OC* and *BSP* are induced between five- and eightfold.

To address the possibility of the direct regulation of osteoblast genes, we tested the competency of HOXA10 to induce their expression independent of RUNX2 by using a TERT-immortalized preosteoblastic cell line derived from *Runx2* null mice (1) (Fig. 9C). Cells were transfected with *Hoxa10* and/or *Runx2* expression vector, and total cellular RNA was analyzed 24 h later. Expression profiling by real-time PCR revealed that HOXA10 induced *OC*, *ALP*, and *BSP* to an extent the same as that seen for their induction by RUNX2 (three- to fourfold for *OC* or *BSP* and five- to sixfold for *ALP*). The presence of HOXA10 and RUNX2 together resulted in an additive induction for *OC* and *BSP*, genes whose expression continues to increase during differentiation (Fig. 7 and 8), but not *ALP* (Fig. 8).

HOXA10 activation of osteogenic genes *OC*, *ALP*, and *BSP* in *Runx2* null cells, taken together with the association of HOXA10 with binding elements in these promoters, supports a RUNX2-independent direct role for HOXA10 in promoting osteoblast differentiation. However, these promoters are also *Runx2* responsive, and HOXA10 directly induces *Runx2*, thereby contributing to HOXA10 RUNX2-dependent transcription of osteoblast genes. The BMP2-initiated induction of *Hoxa10*, *Runx2*, and other transcriptional factors (e.g., DLX3 and DLX5) indicates that these factors all contribute specific regulatory functions to support bone formation. This combinatorial control is schematically illustrated in Fig. 9D.

HOXA10 contributes to chromatin modification of osteoblast target genes for induced transcription. The early recruitment of HOXA10, prior to RUNX2, on the *OC*, *ALP*, and *BSP* gene promoters suggests that HOXA10 may contribute to remodeling the chromatin of these phenotypic genes. The re-

modeling of chromatin structure is mediated in part by enzymes that topologically alter DNA interactions with histones or that covalently modify the core histone proteins H3 and H4 (41). Acetylation of histone H4 and H3K4 methylation are modifications that strongly correlate with transcriptionally active chromatin (10, 75, 77). To test this hypothesis, we examined the effects of *Hoxa10* depletion on histone acetylation and H3K4 methylation of gene promoters, which reflect transcriptionally active chromatin. Cells were treated with *Hoxa10*-specific siRNA for 72 h (Fig. 10A), and these chromatin modifications were assayed by ChIP analysis for the four bone phenotypic genes (Fig. 10B). We confirmed a 50% knockdown of *Hoxa10* by siRNA and a 50% reduction in HOXA10 binding to *OC*, *ALP*, and *BSP* promoters but a modest decrease in the recruitment of HOXA10 to the RUNX2 promoter (Fig. 10B, left panels). We observed a significant 50% reduction in the acetylation of *OC*, *BSP*, and *Runx2* chromatin but a modest decrease in *ALP* chromatin acetylation in cells treated with *Hoxa10* siRNA relative to control levels (nonsilencing siRNA) (Fig. 10B). On the other hand, we found in multiple studies (*n* = 3) a significant decrease in the H3K4 methylation of *ALP* and *BSP*, while the methylation of *OC* and *Runx2* chromatin was less decreased.

Upon RNAi-mediated depletion of HOXA10, we found an impairment of histone modifications in the chromatin of the *Runx2*, *OC*, *ALP*, and *BSP* genes, suggesting that coregulatory proteins with histone acetyltransferase (HAT) activity may be present in a HOXA10 complex associated with chromatin. To address this mechanism of chromatin remodeling by HOXA10 binding to target genes, we examined the association of coregulatory proteins having HAT activity, p300 and CBP, with HOXA10 (Fig. 10C). We performed sequential chromatin immunoprecipitation studies (ChIP-reChIP) to determine the in vivo interactions of HOXA10 with coactivator proteins on the

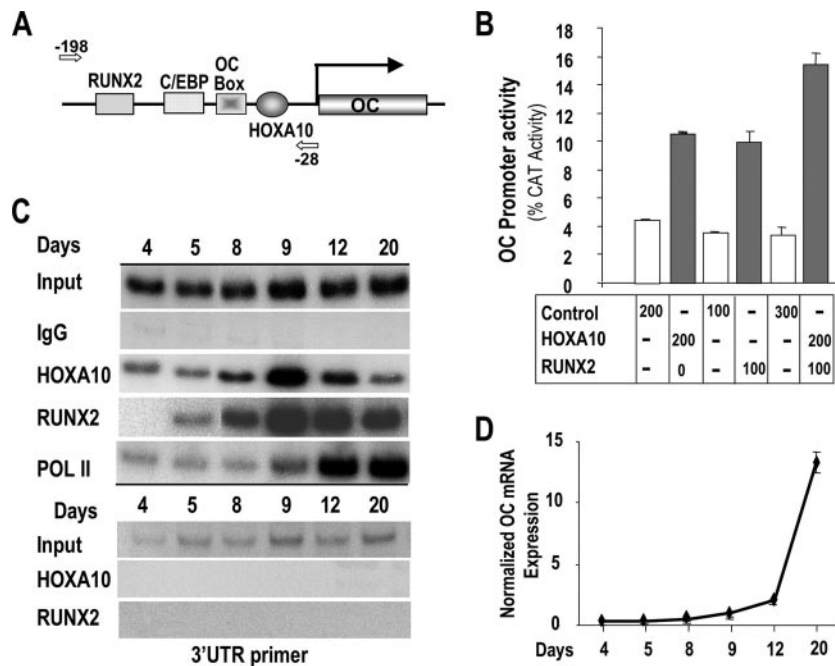


FIG. 7. HOXA10 is recruited to the *OC* promoter to directly regulate gene expression. (A) Activation of *OC* gene transcription by HOXA10. Schematic representation of rat proximal *OC* promoter segment illustrating the location of the only *Hoxa10* consensus motif in the -208 -bp $5'$ *OC* fragment. Arrows are the forward (-198) and reverse (-28) *OC* primers used in ChIP analysis. (B) The mouse preosteoblast cell line MC3T3-E1 was cotransfected with either empty vector (control) or *Hoxa10* and *Runx2* expression plasmids as indicated and with the proximal *OC* promoter (-208 OC-CAT) by use of FuGENE6 (Roche Molecular Biologicals). Control cells contained the indicated amount of backbone plasmid (*pGL3*). Cells were harvested 24 h posttransfection for CAT assay. Promoter activity was calculated from values equivalent to those for six samples and expressed as percent CAT activity. (C) In vivo occupancy of HOXA10 on the *OC* gene. Cross-linked chromatin samples from primary rat calvarium-derived osteoblast cultures at the indicated stages of differentiation (days 4, 5, 8, 9, 12, and 20) were used for immunoprecipitation reactions with $2 \mu\text{g}$ of HOXA10, RUNX2, Pol II, and nonspecific antibody (IgG). The pull-down DNA fragments were purified and assayed by PCR. Input represents 1% of each chromatin fraction used for immunoprecipitation. The ChIP data presented are representative of multiple experiments in which all the time point data were derived from the same osteoblast preparation. The lower panel shows the control for ChIP primer specificity. (D) Expression of *OC* mRNA (QPCR) during differentiation of primary calvarial osteoblasts at the indicated days. C/EBP, CCAAT/enhancer-binding proteins.

Runx2 and *OC* promoters in ROS 17/2.8 cells. These cells robustly express endogenous bone-related factors. A first ChIP was performed with HOXA10 antibody, followed by pull-down with antibodies specific to each coregulatory protein (Fig. 10C). Although the interaction of HOXA10 is greater with the *OC* gene than with the *Runx2* promoter, p300 and CBP are found in the HOXA10 complex associated with both genes. These results demonstrate that the presence of HOXA10 on bone target genes can contribute to epigenetic alterations in chromatin that favor transcription (summarized in Fig. 10D).

DISCUSSION

In this study we have defined a principal role for HOXA10 in contributing to osteoblast cell fate and differentiation. *Hoxa10*, which is essential for skeletal patterning, is characterized in our studies as an activator of *Runx2* and three phenotypic genes (*ALP*, *BSP*, and *OC*) that represent progressive stages of osteoblastogenesis. Our data support the concept that HOXA10 functions in initiating osteogenic gene expression but that the bone phenotype is not fully established until *Runx2* is expressed. The evidence includes the following: (i) the finding that *Hoxa10* and *Runx2* are immediate-response genes to the BMP2 morphogenetic signal and exhibit similar expression

profiles during the induction of the osteoblast phenotype in C2C12 cells; (ii) the exhibition by both genes of robust expression in osteoprogenitors, growth plate chondrocytes, and osteoblasts in vivo, which further demonstrates the coexpression of HOXA10 and RUNX2 in osteogenic lineage cells in vivo; (iii) the activation of *Runx2* transcription by HOXA10 in mesenchymal cells; (iv) the early recruitment of HOXA10 to target gene chromatin during induction of the osteoblast phenotype, which has consequential effects on acetylation and H3K4 methylation, a signature of active chromatin; and (v) RNAi-directed depletion and exogenous expression of HOXA10, which confirm a coordinate change in endogenous expression of *Runx2* and osteoblast genes. Further, the demonstration that HOXA10 can directly regulate osteogenic genes in the absence of *Runx2* (studies performed with *Runx2*^{-/-} cells) identifies HOXA10 as a contributor to bone formation independent of *Runx2*. Together, these results indicate that HOXA10 plays a pivotal role at the onset of osteoblast commitment and may be a significant factor in contributing to osteoblastogenesis by dynamic regulation of osteoblast genes throughout stages of differentiation. Thus, *Hoxa10* has a key role in promoting bone tissue formation beyond its requirement for patterning the embryonic skeleton.

Our findings suggest HOXA10 functions in a linear pathway

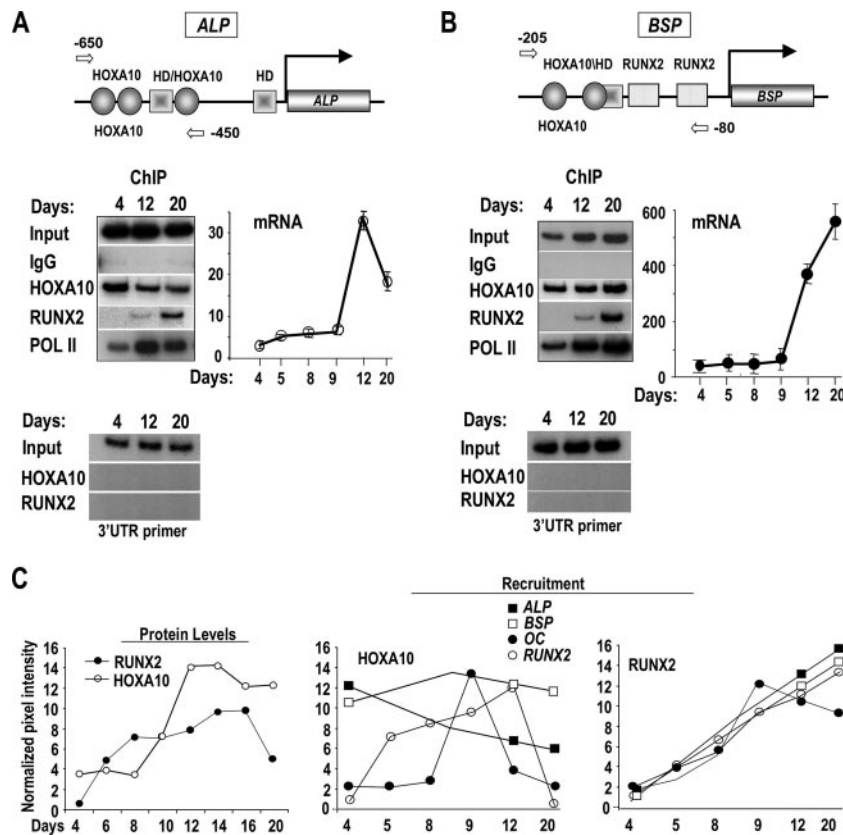


FIG. 8. *Hoxa10* regulatory elements are present in the *ALP* (A) and *BSP* (B) genes. ChIP assay was performed with primary rat calvarial osteoblasts by use of the indicated antibodies at the proliferation stage (day 4) and the differentiation stages (days 12 and 20, early and mature osteoblasts in mineralized matrix). HD, homeodomain. (Top) Illustration of *Hoxa10* sites and locations of primers (arrows) used to detect the association of HOXA10 with the *ALP* and *BSP* promoters; (bottom) ChIP quantitated by radioactivity with control primers shown below (left) and expression of *ALP* and *BSP* genes by RT-PCR (right). (C) Summary profiles of cell protein levels and recruitment of HOXA10 and RUNX2 to four bone promoters. The data represent densitometric values obtained from Western blot and ChIP experiments normalized to actin and IgG values, respectively.

with RUNX2 to promote bone formation as well as independently of RUNX2. Our model (Fig. 9D) proposes that HOXA10 functions as an immediate early response gene to the BMP2 signal for the initiation of osteogenic gene regulation and provides an amplification step for RUNX2-induced expression to establish the osteoblast phenotype. As other BMP2-induced transcription factors regulate *Runx2* and osteoblastic genes (e.g., homeodomain proteins [MSX2, DLX3, and DLX5], TCF/LEF1, AP-1, OSTERIX, CCAAT/enhancer-binding proteins [encoded by *C/EBP*], and ATF4) (22, 28, 45, 82, 83, 86), a compelling question is that of the hierarchy of HOXA10, RUNX2, and these other factors in regulating gene expression for bone formation. Null mouse models have identified OSTERIX function later than RUNX2 (56). From a developmental perspective, BMP/TGF β , Wnt, and HOX signaling interactions are documented (5, 62), and all of these proteins contribute to bone development. From a gene regulation perspective, a hierarchy of transcriptional control can be better deduced by understanding the ordered recruitment of factors to gene promoters and the temporal levels of the regulatory factors during osteoblast differentiation. Abd B class *Hoxa10*, *Msx2*, and the distal-less *Dlx3* genes are induced within a few hours, while other factors (e.g., *Dlx5* and *C/EBP)*

are induced later (after 8 h) in the C2C12 model. Recent studies provide evidence from ChIP studies for a homeodomain protein regulatory network for osteoblast commitment and differentiation (35). Here we show HOXA10 to be associated with bone promoters prior to RUNX2, suggesting that it contributes to the initiation of the osteoblast phenotype. However, increased HOXA10 binding appears to be coordinated with increased recruitment of *Runx2*, homeodomain proteins, and other factors postproliferatively for accumulation of mRNA, thereby establishing the bone phenotype (35). The selective temporal binding of HOXA10 to promoters reflects binding and dissociation during differentiation. This is in contrast to the continual increase in RUNX2 binding to promoters, suggesting that HOXA10 has a very dynamic regulatory function for regulating osteogenic gene expression during osteoblast differentiation.

We found modifications of histones at the level of chromatin in response to altered HOXA10 expression, indicating a remodeling of the transcriptional machinery that is necessary for in vivo gene regulation. HOXA10 recruitment to bone promoters prior to a significant accumulation of mRNA but after Pol II association emphasizes a functional role for HOXA10 increasing transcription through chromatin remodeling. This is

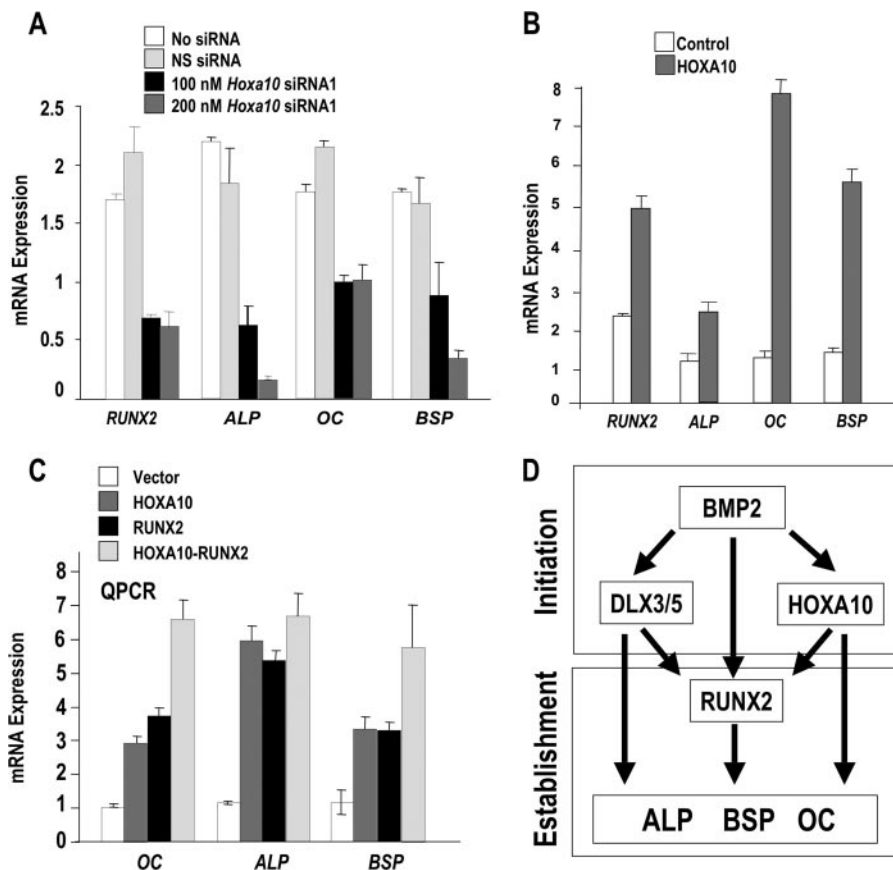


FIG. 9. HOXA10 regulation of osteoblast phenotypic genes dependent on and independent of RUNX2. (A) Transcript levels of bone phenotypic markers are decreased by *Hoxa10* siRNA treatment at the indicated doses. RT-QPCR mRNA expression profiles in *Hoxa10* siRNA-treated (100 and 200 nM) MC3T3 cells. The relative mRNA expression profiles of the endogenous marker genes were normalized to *Gapdh* expression profiles. Error bars are means \pm standard deviations from triplicate samples. (B) Forced expression of *Hoxa10* (200 ng) for 24 h induces expression of bone phenotypic genes (RT-QPCR analyses of six samples). (C) A *Runx2*^{-/-} TERT-immortalized stable cell line was transfected with 400 ng cytomegalovirus-driven *Hoxa10*, 200 ng *Runx2*, or both expression plasmids for 24 to 36 h (six samples). Cell layers were harvested for total cellular RNA and analyzed for expression of indicated genes by RT-QPCR. (D) Schematic illustration of the BMP2-induced HOXA10, homeodomain proteins DLX3/DLX5, and RUNX2 gene expression representing the initiation phase of osteogenesis. Together these genes establish the osteoblast phenotype by direct and Runx2-dependent activities on target genes.

supported by knockdown of HOXA10 reducing histone acetylation and H3K4 methylation, which are associated with active transcription and by HOXA10 and p300/CBP coassociation on the *Runx2* and *OC* promoters (ChIP-reChIP studies). Earlier studies have reported that HOX factors can modify transcriptional activation and repression by interacting with p300/CBP (14, 71). Our studies have focused on HOXA10 in supporting chromatin remodeling for the activation of osteoblast-related genes, as was shown for p21 (9). Equally important is the fact that HOXA10 can promote histone deacetylation by recruiting histone deacetylase 2 and SIRT2 histone deacetylases to repress gene transcription (67). Histone deacetylase-HOXA10 interactions would reverse HAT activity and could be operative in osteoblasts for HOXA10 to mediate either activation or attenuation of gene expression. Such mechanisms are important for HOXA10 suppressor function in undifferentiated myeloid cells and HOXA9 regulation of neovascularization (2, 51, 65, 78). In addition to coregulatory factors that modify chromatin, the other well-characterized partner proteins for the Abd B HOX proteins, PBX1 and MEIS, both

having homeodomain protein modules, form complexes with HOX proteins and also bind to DNA to regulate repressor and enhancer activities of *Hox* genes. HOXA9, HOXA10, HOXA11, HOXD12, and HOXB13 each have different properties of interaction with these coregulators (52, 61, 72–74). For example, high-affinity DNA binding can be achieved when HOXB9 and HOXA10 proteins are dimerized with PBX1. While our forced-expression and siRNA knockdown studies show that HOXA10 has anabolic activity on osteoblast gene expression, how these endogenous partner proteins influence the HOXA10-mediated expression of osteoblast genes is a provocative question.

The specificity of HOXA10 for regulating osteoblast differentiation should be considered in relation to *Hox* nonparalogous and paralogous genes, which are known to overlap in expression in some tissues but can have preferential activities (15, 17, 27). For example, HOXA10 and HOXD10 regulate the skeleton but may exhibit specific gene regulation properties (36, 49, 79). Also, HOXA10 and HOX11 homeobox proteins are equivalent for axial but not appendicular skeletal develop-

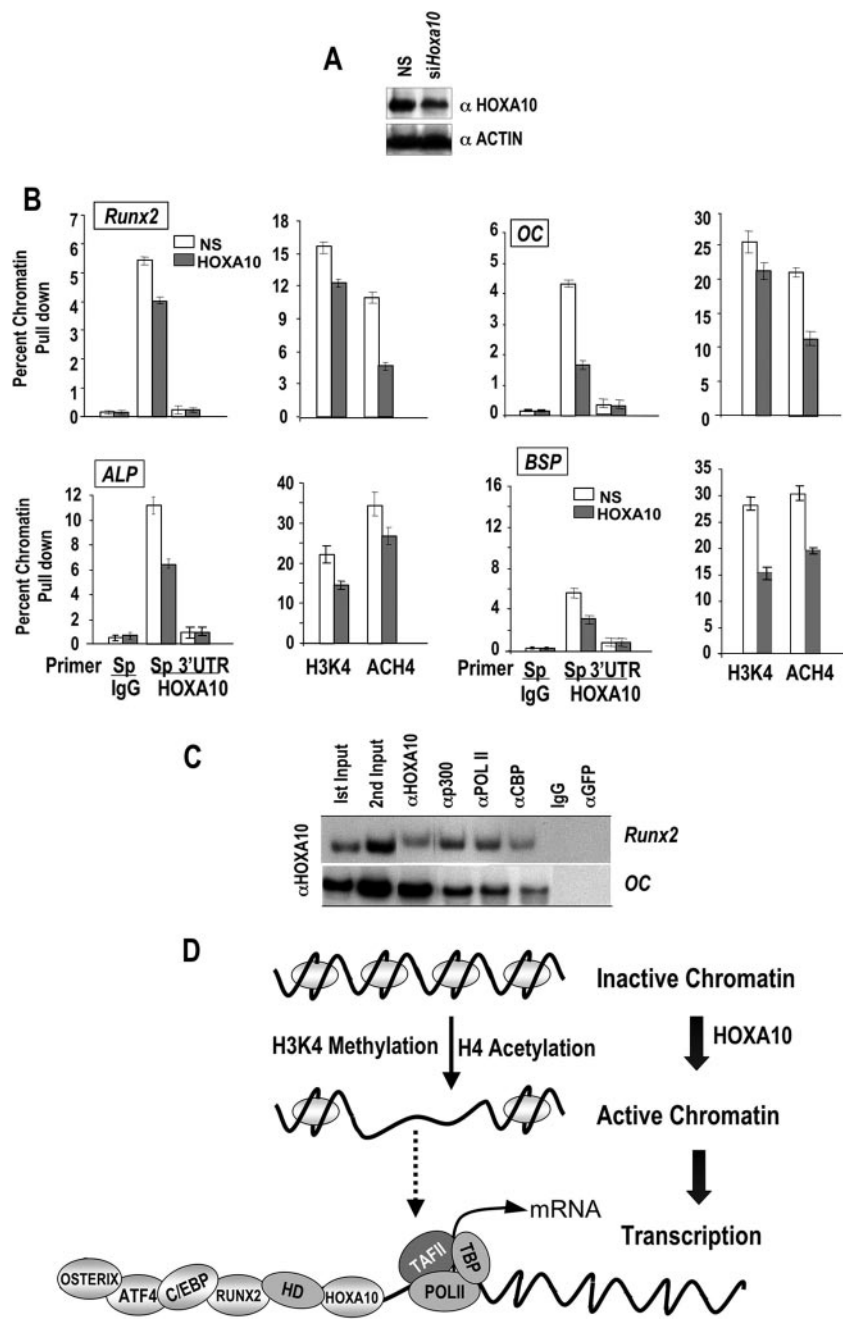


FIG. 10. siRNA knockdown of *Hoxa10* decreases histone acetylation and H3K4 methylation of osteogenic genes. (A) MC3T3 cells were treated with *Hoxa10* siRNA and nonspecific control (NS) for 72 h. The knockdown effect is shown by Western blotting. (B) DNA samples from ChIP with HOXA10, nonspecific IgG, methylated histone K4 (H3K4), and acetylated histone H4 (ACH4) were amplified by gene-specific (Sp) and 3' control UTR primers (Table 1) for the indicated gene promoters. The left panel for each gene shows the effect of *Hoxa10* siRNA on HOXA10 recruitment in ChIP assay of the indicated promoter. The right panel shows the status of H3K4 methylation or H4 acetylation of the chromatin modification by *Hoxa10*-specific knockdown. (C) ChIP-reChIP assays were performed to identify the association of coregulatory factors p300 and CBP with HOXA10 on the *Runx2* and *OC* promoters. A HOXA10 ChIP was performed with HOXA10 antibody, and the resulting chromatin immunoprecipitate (second input) was subjected to reChIP with the indicated antibodies (α) (secondary pull-down). Normal IgG and green fluorescent protein (GFP) antibodies provided controls. The DNA fragments for *Runx2* and *OC* were amplified as described in Materials and Methods. (D) Schematic illustration to show how HOXA10 belongs to an epigenetic coregulatory complex for remodeling chromatin to induce transcription of osteogenic genes. We propose that HOXA10 may be among the earliest factors recruited to bone promoters. HOXA10 recruitment is followed by the coordinated occupancy of other bone-related transcription factors for maximal expression of individual genes during stages of differentiation. HD, homeodomain.

ment (87). The TTAT regulatory element is recognized by several HOX proteins; however, protein-DNA interactions as well as protein-protein interactions are dependent on the contextual sequence of the core TTAT motif (8, 13, 57). Our analysis of the functional specificity of the *Runx2 Hoxa10* site 1 and no other core motifs in the 0.6-kb *Runx2* promoter is consistent with other studies evaluating the specificities of *Hoxa10* sites (4, 72, 74). Although several HOX proteins are likely present in osteoblast nuclear extracts (e.g., HOXA9), our findings revealed a supershifted/block shifted complex by the HOXA10 antibody. However, it is possible that other HOX protein interactions may occur at this and potentially other HOX motifs within the *Runx2* gene. Our data do support the concept that the *Runx2* site 1 (TTAT) has a high degree of specificity for HOXA10 binding. Interestingly, the *OC* gene is characterized by a TTAC core motif, implicating this motif in the formation of complexes that support a high degree of OC expression in mature osteoblasts. It is also noteworthy that the flanking nucleotides are distinct among the four target genes studied here (Table 2). This finding implies that their sequences may hold information for the dynamic association of HOXA10 with an individual gene throughout differentiation.

HOXA10 is expressed in many different tissues in which its functions have been addressed and may be related to its activities in bone tissue. Progesterone and 17 β -estradiol, hormones that regulate turnover of adult bone (53, 63), increase *Hoxa10* expression (16, 48). HOXA10 regulates hematopoietic differentiation in part via activation of p21 (WAF1/CIP1), the cyclin-dependent kinase inhibitor (9, 25). In the spinal cord, expression of *Hoxa10* is confined to the postmitotic cell population (15). We find that HOXA10 is expressed in proliferating cells and upregulated in postproliferative mature osteoblasts in vitro. HOXA10 is also a target of induction by vitamin D₃ (66), a hormone that increases the expression of osteoblast-related genes. Thus, HOXA10 appears to have a broad role in gene regulation for contributing to cell differentiation. Our studies have added to the growing recognition that *Hox* genes have important functions in the adult, including now the skeleton (55).

In conclusion, our characterization of HOXA10 positive regulation of genes that represent major functional components for bone formation, including those encoding RUNX2 (a bone essential transcription factor), alkaline phosphatase (required for matrix mineralization), bone sialoprotein (an important cell matrix-binding phosphoprotein with hydroxyapatite nucleation capabilities), and OC (the calcium binding bone-specific protein) (47), solidifies the concept that HOXA10 is an important regulator of gene expression throughout the progression of bone formation. These novel functions for HOXA10 in regulating target genes for osteoblast differentiation and bone formation in the postnatal skeleton have broad implications for HOXA10 functions in normal bone metabolism and bone-related disorders.

ACKNOWLEDGMENTS

Studies reported were supported in part by grants from the National Institutes of Health (DE12528, AR39588, AR48818, and P30 DK32520).

The contents of this work are solely our responsibility and do not necessarily represent the official views of the National Institutes of Health.

We thank Richard L. Maas (Department of Medicine, Brigham and Women's Hospital, Harvard Medical School, Boston, MA) for reagents, Anthony Imbalzano (University of Massachusetts Medical School) for helpful discussions, Dana Fredericks for technical assistance, and Judy Rask for manuscript preparation.

REFERENCES

- Bae, J.-S., S. Gutierrez, R. Narla, J. Pratap, R. Devados, J. L. Stein, J. B. Lian, G. S. Stein, and A. Javed. 2007. Reconstitution of Runx2/Cbfa1 null cells identifies Runx2 functional domains required for osteoblast differentiation and responsiveness to osteogenic regulators BMP2, TGF α and 1,25(OH)₂D₃. *J. Cell. Biochem.* **100**:434–449.
- Bae, N. S., M. J. Swanson, A. Vassilev, and B. H. Howard. 2004. Human histone deacetylase SIRT2 interacts with the homeobox transcription factor HOXA10. *J. Biochem. (Tokyo)* **135**:695–700.
- Balint, E., D. Lapointe, H. Drissi, C. van der Meijden, D. W. Young, A. J. van Wijnen, J. L. Stein, G. S. Stein, and J. B. Lian. 2003. Phenotype discovery by gene expression profiling: mapping of biological processes linked to BMP-2-mediated osteoblast differentiation. *J. Cell. Biochem.* **89**:401–426.
- Benson, G. V., T. H. Nguyen, and R. L. Maas. 1995. The expression pattern of the murine *Hoxa-10* gene and the sequence recognition of its homeodomain reveal specific properties of *Abdominal B*-like genes. *Mol. Cell. Biol.* **15**:1591–1601.
- Bondos, S. 2006. Variations on a theme: Hox and Wnt combinatorial regulation during animal development. *Sci. STKE* **2006**:e38.
- Boulet, A. M., and M. R. Capecchi. 2002. Duplication of the *Hoxd11* gene causes alterations in the axial and appendicular skeleton of the mouse. *Dev. Biol.* **249**:96–107.
- Boulet, A. M., and M. R. Capecchi. 2004. Multiple roles of *Hoxa11* and *Hoxd11* in the formation of the mammalian forelimb zeugopod. *Development* **131**:299–309.
- Brake, R. L., U. R. Kees, and P. M. Watt. 2002. A complex containing PBX2 contributes to activation of the proto-oncogene HOX11. *Biochem. Biophys. Res. Commun.* **294**:23–34.
- Bromleigh, V. C., and L. P. Freedman. 2000. p21 is a transcriptional target of HOXA10 in differentiating myelomonocytic cells. *Genes Dev.* **14**:2581–2586.
- Bulger, M. 2005. Hyperacetylated chromatin domains: lessons from heterochromatin. *J. Biol. Chem.* **280**:21689–21692.
- Carapuco, M., A. Novoa, N. Bobola, and M. Mallo. 2005. Hox genes specify vertebral types in the presomitic mesoderm. *Genes Dev.* **19**:2116–2121.
- Carpenter, E. M., J. M. Goddard, A. P. Davis, T. P. Nguyen, and M. R. Capecchi. 1997. Targeted disruption of *Hoxd-10* affects mouse hindlimb development. *Development* **124**:4505–4514.
- Chang, C. P., L. Brocchieri, W. F. Shen, C. Largman, and M. L. Cleary. 1996. Pbx modulation of Hox homeodomain amino-terminal arms establishes different DNA-binding specificities across the Hox locus. *Mol. Cell. Biol.* **16**:1734–1745.
- Chariot, A., C. van Lint, M. Chapelier, J. Gielen, M. P. Merville, and V. Bours. 1999. CBP and histone deacetylase inhibition enhance the transactivation potential of the HOXB7 homeodomain-containing protein. *Oncogene* **18**:4007–4014.
- Choe, A., H. Q. Phun, D. D. Tieu, Y. H. Hu, and E. M. Carpenter. 2006. Expression patterns of Hox10 paralogous genes during lumbar spinal cord development. *Gene Expr. Patterns* **6**:730–737.
- Daftary, G. S., and H. S. Taylor. 2006. Endocrine regulation of HOX genes. *Endocr. Rev.* **27**:331–355.
- Davis, A. P., D. P. Witte, H. M. Hsieh-Li, S. S. Potter, and M. R. Capecchi. 1995. Absence of radius and ulna in mice lacking *hoxa-11* and *hoxd-11*. *Nature* **375**:791–795.
- de la Fuente, L., and J. A. Helms. 2005. Head, shoulders, knees, and toes. *Dev. Biol.* **282**:294–306.
- Depew, M. J., C. A. Simpson, M. Morasso, and J. L. Rubenstein. 2005. Reassessing the Dlx code: the genetic regulation of branchial arch skeletal pattern and development. *J. Anat.* **207**:501–561.
- Dobrev, G., M. Chahrouh, M. Dautzenberg, L. Chirivella, B. Kanzler, I. Farinas, G. Karsenty, and R. Grosschedl. 2006. SATB2 is a multifunctional determinant of craniofacial patterning and osteoblast differentiation. *Cell* **125**:971–986.
- Drissi, H., Q. Luc, R. Shakoobi, S. Chuva de Sousa Lopes, J.-Y. Choi, A. Terry, M. Hu, S. Jones, J. C. Neil, J. B. Lian, J. L. Stein, A. J. van Wijnen, and G. S. Stein. 2000. Transcriptional autoregulation of the bone related CBFA1/RUNX2 gene. *J. Cell. Physiol.* **184**:341–350.
- Drissi, H., A. Pouliot, J. L. Stein, A. J. van Wijnen, G. S. Stein, and J. B. Lian. 2002. Identification of novel protein/DNA interactions within the promoter of the bone-related transcription factor Runx2/Cbfa1. *J. Cell. Biochem.* **86**:403–412.
- Ducy, P., R. Zhang, V. Geoffroy, A. L. Ridall, and G. Karsenty. 1997. Osf2/Cbfa1: a transcriptional activator of osteoblast differentiation. *Cell* **89**:747–754.
- Ekker, S. C., D. G. Jackson, D. P. von Kessler, B. I. Sun, K. E. Young, and

- P. A. Beachy. 1994. The degree of variation in DNA sequence recognition among four *Drosophila* homeotic proteins. *EMBO J.* **13**:3551–3560.
25. Eklund, E. A. 2006. The role of HOX genes in myeloid leukemogenesis. *Curr. Opin. Hematol.* **13**:67–73.
 26. Favier, B., F. M. Rijli, C. Fromental-Ramain, V. Fraulob, P. Chambon, and P. Dolle. 1996. Functional cooperation between the non-paralogous genes *Hoxa-10* and *Hoxd-11* in the developing forelimb and axial skeleton. *Development* **122**:449–460.
 27. Fromental-Ramain, C., X. Warot, S. Lakkaraju, B. Favier, H. Haack, C. Birling, A. Dierich, P. Dollé, and P. Chambon. 1996. Specific and redundant functions of the paralogous *Hoxa-9* and *Hoxd-9* genes in forelimb and axial skeleton patterning. *Development* **122**:461–472.
 28. Gaur, T., C. J. Lengner, H. Hovhannisyan, R. A. Bhat, P. V. N. Bodine, B. S. Komm, A. Javed, A. J. van Wijnen, J. L. Stein, G. S. Stein, and J. B. Lian. 2005. Canonical WNT signaling promotes osteogenesis by directly stimulating RUNX2 gene expression. *J. Biol. Chem.* **280**:33132–33140.
 29. Gaur, T., C. J. Lengner, S. Hussain, B. Trevant, D. Ayers, J. L. Stein, P. V. N. Bodine, B. S. Komm, G. S. Stein, and J. B. Lian. 2006. Secreted frizzled protein 1 regulates Wnt signaling for BMP induced chondrocyte differentiation. *J. Cell. Physiol.* **208**:87–96. [Epub ahead of print.]
 30. Gersch, R. P., F. Lombardo, S. C. McGovern, and M. Hadjiargyrou. 2005. Reactivation of Hox gene expression during bone regeneration. *J. Orthop. Res.* **23**:882–890.
 31. Goodman, F. R. 2002. Limb malformations and the human HOX genes. *Am. J. Med. Genet.* **112**:256–265.
 32. Gutierrez, S., A. Javed, D. Tennant, M. van Rees, M. Montecino, G. S. Stein, J. L. Stein, and J. B. Lian. 2002. CCAAT/enhancer-binding proteins (C/EBP) β and δ activate osteocalcin gene transcription and synergize with Runx2 at the C/EBP element to regulate bone-specific expression. *J. Biol. Chem.* **277**:1316–1323.
 33. Harris, S. E., D. Guo, M. A. Harris, A. Krishnaswamy, and A. Lichtler. 2003. Transcriptional regulation of BMP-2 activated genes in osteoblasts using gene expression microarray analysis: role of *Dlx2* and *Dlx5* transcription factors. *Front. Biosci.* **8**:s1249–s1265.
 34. Hassan, M. Q., A. Javed, M. I. Morasso, J. Karlin, M. Montecino, A. J. van Wijnen, G. S. Stein, J. L. Stein, and J. B. Lian. 2004. *Dlx3* transcriptional regulation of osteoblast differentiation: temporal recruitment of *Msx2*, *Dlx3*, and *Dlx5* homeodomain proteins to chromatin of the osteocalcin gene. *Mol. Cell. Biol.* **24**:9248–9261.
 35. Hassan, M. Q., R. S. Tare, S. Lee, M. Mandeville, M. I. Morasso, A. Javed, A. J. van Wijnen, J. L. Stein, G. S. Stein, and J. B. Lian. 2006. BMP2 commitment to the osteogenic lineage involves activation of Runx2 by *Dlx3* and a homeodomain transcriptional network. *J. Biol. Chem.* **281**:40515–40526.
 36. Hedlund, E., S. L. Karsten, L. Kudo, D. H. Geschwind, and E. M. Carpenter. 2004. Identification of a *Hoxd10*-regulated transcriptional network and combinatorial interactions with *Hoxa10* during spinal cord development. *J. Neurosci. Res.* **75**:307–319.
 37. Hoffmann, H. M., T. L. Beumer, S. Rahman, L. R. McCabe, C. Banerjee, F. Aslam, J. A. Tiro, A. J. van Wijnen, J. L. Stein, G. S. Stein, and J. B. Lian. 1996. Bone tissue-specific transcription of the osteocalcin gene: role of an activator osteoblast-specific complex and suppressor hox proteins that bind the OC box. *J. Cell. Biochem.* **61**:310–324.
 38. Izpisua-Belmonte, J. C., H. Falkenstein, P. Dolle, A. Renucci, and D. Duboule. 1991. Murine genes related to the *Drosophila* *AbdB* homeotic genes are sequentially expressed during development of the posterior part of the body. *EMBO J.* **10**:2279–2289.
 39. Javed, A., B. Guo, S. Hiebert, J.-Y. Choi, J. Green, S.-C. Zhao, M. A. Osborne, S. Stifani, J. L. Stein, J. B. Lian, A. J. van Wijnen, and G. S. Stein. 2000. Groucho/TLE/R-Esp proteins associate with the nuclear matrix and repress RUNX (CBF α /AML/PEBP2 α) dependent activation of tissue-specific gene transcription. *J. Cell Sci.* **113**:2221–2231.
 40. Javed, A., S. Gutierrez, M. Montecino, A. J. van Wijnen, J. L. Stein, G. S. Stein, and J. B. Lian. 1999. Multiple *Cbfa*/AML sites in the rat osteocalcin promoter are required for basal and vitamin D responsive transcription and contribute to chromatin organization. *Mol. Cell. Biol.* **19**:7491–7500.
 41. Jenuwein, T., and C. D. Allis. 2001. Translating the histone code. *Science* **293**:1074–1080.
 42. Kim, Y. J., H. N. Kim, E. K. Park, B. H. Lee, H. M. Ryoo, S. Y. Kim, I. S. Kim, J. L. Stein, J. B. Lian, G. S. Stein, A. J. van Wijnen, and J. Y. Choi. 2006. The bone-related Zn finger transcription factor Osterix promotes proliferation of mesenchymal cells. *Gene* **366**:145–151.
 43. Komori, T., H. Yagi, S. Nomura, A. Yamaguchi, K. Sasaki, K. Deguchi, Y. Shimizu, R. T. Bronson, Y.-H. Gao, M. Inada, M. Sato, R. Okamoto, Y. Kitamura, S. Yoshiki, and T. Kishimoto. 1997. Targeted disruption of *Cbfa1* results in a complete lack of bone formation owing to maturational arrest of osteoblasts. *Cell* **89**:755–764.
 44. Krumlauf, R. 1994. Hox genes in vertebrate development. *Cell* **78**:191–201.
 45. Lee, M. H., Y. J. Kim, W. J. Yoon, J. I. Kim, B. G. Kim, Y. S. Hwang, J. M. Wozney, X. Z. Chi, S. C. Bae, K. Y. Choi, J. Y. Cho, J. Y. Choi, and H. M. Ryoo. 2005. *Dlx5* specifically regulates Runx2-II expression by binding to homeodomain response elements in the Runx2 distal promoter. *J. Biol. Chem.* **280**:35579–35587.
 46. Lengner, C. J., M. Q. Hassan, R. W. Serra, C. Lepper, A. J. van Wijnen, J. L. Stein, J. B. Lian, and G. S. Stein. 2005. Nkx3.2 mediated repression of RUNX2 promotes chondrogenic differentiation. *J. Biol. Chem.* **280**:15872–15879.
 47. Lian, J. B., A. Javed, S. K. Zaidi, C. Lengner, M. Montecino, A. J. van Wijnen, J. L. Stein, and G. S. Stein. 2004. Regulatory controls for osteoblast growth and differentiation: role of Runx/Cbfa/AML factors. *Crit. Rev. Eukaryot. Gene Expr.* **14**:1–41.
 48. Lim, H., L. Ma, W. G. Ma, R. L. Maas, and S. K. Dey. 1999. *Hoxa-10* regulates uterine stromal cell responsiveness to progesterone during implantation and decidualization in the mouse. *Mol. Endocrinol.* **13**:1005–1017.
 49. Lin, A. W., and E. M. Carpenter. 2003. *Hoxa10* and *Hoxd10* coordinately regulate lumbar motor neuron patterning. *J. Neurobiol.* **56**:328–337.
 50. Lowney, P., J. Corral, K. Detmer, M. M. LeBeau, L. Deaven, H. J. Lawrence, and C. Largman. 1991. A human Hox 1 homeobox gene exhibits myeloid-specific expression of alternative transcripts in human hematopoietic cells. *Nucleic Acids Res.* **19**:3443–3449.
 51. Lu, Y., I. Goldenberg, L. Bei, J. Andrejic, and E. A. Eklund. 2003. *HoxA10* represses gene transcription in undifferentiated myeloid cells by interaction with histone deacetylase 2. *J. Biol. Chem.* **278**:47792–47802.
 52. Mann, R. S., and M. Affolter. 1998. Hox proteins meet more partners. *Curr. Opin. Genet. Dev.* **8**:423–429.
 53. Manolagas, S. C., S. Kousteni, and R. L. Jilka. 2002. Sex steroids and bone. *Recent Prog. Horm. Res.* **57**:385–409.
 54. Merabet, S., J. Pradel, and Y. Graba. 2005. Getting a molecular grasp on Hox contextual activity. *Trends Genet.* **21**:477–480.
 55. Morgan, R. 2006. Hox genes: a continuation of embryonic patterning? *Trends Genet.* **22**:67–69.
 56. Nakashima, K., X. Zhou, G. Kunkel, Z. Zhang, J. M. Deng, R. R. Behringer, and B. de Crombrughe. 2002. The novel zinc finger-containing transcription factor osterix is required for osteoblast differentiation and bone formation. *Cell* **108**:17–29.
 57. Neuteboom, S. T., and C. Murre. 1997. Pbx raises the DNA binding specificity but not the selectivity of antennapedia Hox proteins. *Mol. Cell. Biol.* **17**:4696–4706.
 58. Otto, F., A. P. Thornell, T. Crompton, A. Denzel, K. C. Gilmour, I. R. Rosewell, G. W. H. Stamp, R. S. P. Beddington, S. Mundlos, B. R. Olsen, P. B. Selby, and M. J. Owen. 1997. *Cbfa1*, a candidate gene for cleidocranial dysplasia syndrome, is essential for osteoblast differentiation and bone development. *Cell* **89**:765–771.
 59. Owen, T. A., M. Aronow, V. Shalhoub, L. M. Barone, L. Wilming, M. S. Tassinari, M. B. Kennedy, S. Pockwinse, J. B. Lian, and G. S. Stein. 1990. Progressive development of the rat osteoblast phenotype in vitro: reciprocal relationships in expression of genes associated with osteoblast proliferation and differentiation during formation of the bone extracellular matrix. *J. Cell. Physiol.* **143**:420–430.
 60. Pineault, N., C. Abramovich, H. Ohta, and R. K. Humphries. 2004. Differential and common leukemogenic potentials of multiple NUP98-Hox fusion proteins alone or with Meis1. *Mol. Cell. Biol.* **24**:1907–1917.
 61. Pineault, N., C. D. Helgason, H. J. Lawrence, and R. K. Humphries. 2002. Differential expression of Hox, Meis1, and Pbx1 genes in primitive cells throughout murine hematopoietic ontogeny. *Exp. Hematol.* **30**:49–57.
 62. Pockwinse, S. M., J. B. Lawrence, R. H. Singer, J. L. Stein, J. B. Lian, and G. S. Stein. 1993. Gene expression at single cell resolution associated with development of the bone cell phenotype: ultrastructural and in situ hybridization analysis. *Bone* **14**:347–352.
 63. Riggs, B. L., S. Khosla, and L. J. Melton III. 2002. Sex steroids and the construction and conservation of the adult skeleton. *Endocr. Rev.* **23**:279–302.
 64. Rijli, F. M., and P. Chambon. 1997. Genetic interactions of Hox genes in limb development: learning from compound mutants. *Curr. Opin. Genet. Dev.* **7**:481–487.
 65. Rossig, L., C. Urbich, T. Brühl, E. Dernbach, C. Heeschen, E. Chavakis, K. Sasaki, D. Aicher, F. Diehl, F. Seeger, M. Potente, A. Aicher, L. Zanetta, E. Dejana, A. M. Zeiher, and S. Dimmeler. 2005. Histone deacetylase activity is essential for the expression of *HoxA9* and for endothelial commitment of progenitor cells. *J. Exp. Med.* **201**:1825–1835.
 66. Rots, N. Y., M. Liu, E. C. Anderson, and L. P. Freedman. 1998. A differential screen for ligand-regulated genes: identification of *HoxA10* as a target of vitamin D₃ induction in myeloid leukemic cells. *Mol. Cell. Biol.* **18**:1911–1918.
 67. Saleh, M., I. Rambaldi, X. J. Yang, and M. S. Featherstone. 2000. Cell signaling switches HOX-PBX complexes from repressors to activators of transcription mediated by histone deacetylases and histone acetyltransferases. *Mol. Cell. Biol.* **20**:8623–8633.
 68. Salsi, V., and V. Zappavigna. 2006. *Hoxd13* and *Hoxa13* directly control the expression of the EphA7 ephrin tyrosine kinase receptor in developing limbs. *J. Biol. Chem.* **281**:1992–1999.
 69. Shao, J. S., S. L. Cheng, J. M. Pingsterhaus, N. Charlton-Kachigian, A. P.

- Loewy, and D. A. Towler. 2005. Msx2 promotes cardiovascular calcification by activating paracrine Wnt signals. *J. Clin. Invest.* **115**:1210–1220.
70. Shen, J., M. A. Montecino, J. B. Lian, G. S. Stein, A. J. van Wijnen, and J. L. Stein. 2002. Histone acetylation *in vivo* at the osteocalcin locus is functionally linked to vitamin D-dependent, bone tissue-specific transcription. *J. Biol. Chem.* **277**:20284–20292.
 71. Shen, W. F., K. Krishnan, H. J. Lawrence, and C. Largman. 2001. The HOX homeodomain proteins block CBP histone acetyltransferase activity. *Mol. Cell. Biol.* **21**:7509–7522.
 72. Shen, W. F., J. C. Montgomery, S. Rozenfeld, J. J. Moskow, H. J. Lawrence, A. M. Buchberg, and C. Largman. 1997. AbdB-like Hox proteins stabilize DNA binding by the Meis1 homeodomain proteins. *Mol. Cell. Biol.* **17**:6448–6458.
 73. Shen, W. F., S. Rozenfeld, A. Kwong, L. G. Kömüves, H. J. Lawrence, and C. Largman. 1999. HOXA9 forms triple complexes with PBX2 and MEIS1 in myeloid cells. *Mol. Cell. Biol.* **19**:3051–3061.
 74. Shen, W. F., S. Rozenfeld, H. J. Lawrence, and C. Largman. 1997. The Abd-B-like Hox homeodomain proteins can be subdivided by the ability to form complexes with Pbx1a on a novel DNA target. *J. Biol. Chem.* **272**:8198–8206.
 75. Sims, R. J., III, and D. Reinberg. 2006. Histone H3 Lys 4 methylation: caught in a bind? *Genes Dev.* **20**:2779–2786.
 76. Smith, N., Y. Dong, J. Pratap, J. B. Lian, P. Kingsley, A. J. van Wijnen, J. L. Stein, E. M. Schwarz, R. J. O'Keefe, G. S. Stein, and M. H. Drissi. 2005. Overlapping expression of Runx1(Cbfa2) and Runx2(Cbfa1) transcription factors supports cooperative induction of skeletal development. *J. Cell. Physiol.* **203**:133–143.
 77. Sterner, D. E., and S. L. Berger. 2000. Acetylation of histones and transcription-related factors. *Microbiol. Mol. Biol. Rev.* **64**:435–459.
 78. Thorsteinsdottir, U., G. Sauvageau, M. R. Hough, W. Dragowska, P. M. Lansdorp, H. J. Lawrence, C. Largman, and R. K. Humphries. 1997. Overexpression of HOXA10 in murine hematopoietic cells perturbs both myeloid and lymphoid differentiation and leads to acute myeloid leukemia. *Mol. Cell. Biol.* **17**:495–505.
 79. Wahba, G. M., S. L. Hostikka, and E. M. Carpenter. 2001. The paralogous Hox genes Hoxa10 and Hoxd10 interact to pattern the mouse hindlimb peripheral nervous system and skeleton. *Dev. Biol.* **231**:87–102.
 80. Wellik, D. M., and M. R. Capecchi. 2003. Hox10 and Hox11 genes are required to globally pattern the mammalian skeleton. *Science* **301**:363–367.
 81. Williams, T. M., M. E. Williams, and J. W. Innis. 2005. Range of HOX/TALE superclass associations and protein domain requirements for HOXA13:MEIS interaction. *Dev. Biol.* **277**:457–471.
 82. Xiao, G., D. Jiang, C. Ge, Z. Zhao, Y. Lai, H. Boules, M. Phimpilai, X. Yang, G. Karsenty, and R. T. Franceschi. 2005. Cooperative interactions between activating transcription factor 4 and Runx2/Cbfa1 stimulate osteoblast-specific osteocalcin gene expression. *J. Biol. Chem.* **280**:30689–30696.
 83. Yang, X., and G. Karsenty. 2004. ATF4, the osteoblast accumulation of which is determined post-translationally, can induce osteoblast-specific gene expression in non-osteoblastic cells. *J. Biol. Chem.* **279**:47109–47114.
 84. Yoon, B. S., and K. M. Lyons. 2004. Multiple functions of BMPs in chondrogenesis. *J. Cell. Biochem.* **93**:93–103.
 85. Zaidi, S. K., A. Javed, J.-Y. Choi, A. J. van Wijnen, J. L. Stein, J. B. Lian, and G. S. Stein. 2001. A specific targeting signal directs Runx2/Cbfa1 to subnuclear domains and contributes to transactivation of the osteocalcin gene. *J. Cell. Sci.* **114**:3093–3102.
 86. Zambotti, A., H. Makhlef, J. Shen, and P. Ducy. 2002. Characterization of an osteoblast-specific enhancer element in the CBFA1 gene. *J. Biol. Chem.* **277**:41497–41506.
 87. Zhao, Y., and S. S. Potter. 2002. Functional comparison of the Hoxa 4, Hoxa 10, and Hoxa 11 homeoboxes. *Dev. Biol.* **244**:21–36.